2-1-2021

Evaluating cognitive relationships with resting-state and task-driven blood oxygen level-dependent variability

Peter R Millar

Beau M Ances

Brian A Gordon

Tammie L S Benzinger

John C Morris

See next page for additional authors

Authors
Peter R Millar, Beau M Ances, Brian A Gordon, Tammie L S Benzinger, John C Morris, and David A Balota

Evaluating Cognitive Relationships with Resting-State and Task-driven Blood Oxygen Level-Dependent Variability

Peter R. Millar, Beau M. Ances, Brian A. Gordon, Tammie L. S. Benzinger, John C. Morris, and David A. Balota

Abstract

■ Recent functional magnetic resonance imaging studies have reported that moment-to-moment variability in the blood oxygen level-dependent (BOLD) signal is positively associated with task performance and, thus, may reflect a behaviorally sensitive signal. However, it is not clear whether estimates of resting-state and task-driven BOLD variability are differentially related to cognition, as they may be driven by distinct sources of variance in the BOLD signal. Moreover, other studies have suggested that age differences in resting-state BOLD variability may be particularly sensitive to individual differences in cardiovascular, rather than neural, factors. In this study, we tested relationships between measures of behavioral task performance and BOLD variability during both resting-state and task-driven runs of a Stroop and an animacy judgment task in a large, well-characterized sample of cognitively normal middle-aged to older adults. Resting-state BOLD variability was related to composite measures of global cognition and attentional control, but these relationships were eliminated after correction for age or cardiovascular estimates. In contrast, task-driven BOLD variability was related to attentional control measured both inside and outside the scanner, and importantly, these relationships persisted after correction for age and cardiovascular measures. Overall, these results suggest that BOLD variability is a behaviorally sensitive signal. However, resting-state and task-driven estimates of BOLD variability may differ in the degree to which they are sensitive to age-related, cardiovascular, and neural mechanisms. ■

INTRODUCTION

Functional magnetic resonance imaging (fMRI) has provided a powerful tool for cognitive neuroscientists as a noninvasive index of in vivo human brain function. Traditionally, fMRI approaches have focused on mean-level changes in patterns of the blood oxygen level-dependent (BOLD) signal during task performance as a measure of task-related activity. Moreover, there has also been considerable interest in spatial correlation patterns of spontaneous BOLD fluctuation reflecting functional connectivity among brain regions (for a review, see Fox & Raichle, 2007). In addition to these approaches, there is a growing interest in absolute estimates of moment-to-moment variability in the BOLD signal across a run as a potential signal of interest (for a review, see Grady & Garrett, 2014; Garrett, Samanez-Larkin, et al., 2013).

Interest in BOLD variability first emerged in the study of human age differences. Initial studies reported that, in comparison to younger adults, healthy older adults exhibit reduced BOLD variability during brief fixation blocks (Garrett, Kovacevic, McIntosh, & Grady, 2010), task performance (Garrett, Kovacevic, McIntosh, & Grady, 2011), and extended resting-state scans (Kielar et al., 2016). This pattern is somewhat surprising, in part because one early neurocognitive theory of aging predicted that neural variability or noise should increase in older adults (Crossman & Szafran, 1956) and, moreover, that behavioral variability appears to increase with age (for a review, see Balota & Duchek, 2015) and is associated with differences in resting-state networks (Meeker et al., in press; Duchek et al., 2013; Clare Kelly, Uddin, Biswal, Castellanos, & Milham, 2008). Although widespread patterns of age-related reductions in BOLD variability have been observed spanning multiple functional networks, some regional age-related increases in variability have been reported in the same studies. Importantly, these extreme-group (i.e., college-aged students vs. community-dwelling individuals over 60 years old) difference patterns have been replicated in large, continuous aging samples as well (Millar, Petersen, et al., 2020; Nomi, Bolt, Ezie, Uddin, & Heller, 2017; Hu, Chao, Zhang, Ide, & Li, 2014).

In addition to age differences, other studies have examined relationships with task performance, suggesting that task-driven BOLD variability is indeed sensitive to individual differences in performance within the scanner. Specifically, in one study, BOLD variability in occipital, cingulate, angular gyrus, and medial prefrontal regions during perceptual matching, attention cuing, and delayed match-to-sample tasks was positively associated with faster and more consistent reaction time (RT) in those tasks (Garrett et al., 2011). Similar positive relationships between task performance and variability have also been reported in stop signal (Hu et al., 2014), visual working memory (Guitart-Masip et al., 2016), and sensorimotor control, vowel identification, and trait judgment tasks (Grady & Garrett, 2018).

Washington University in St. Louis

Journal of Cognitive Neuroscience 33:2, pp. 279–302
https://doi.org/10.1162/jocn_a_01645

Behavioral relationships have also been demonstrated with resting-state variability. Specifically, greater resting-state low-frequency fluctuations in precuneus and anterior cingulate have been associated with faster and more consistent performance as well as smaller congruency estimates from a flanker task performed in a separate task run (Mennes et al., 2011). Furthermore, in a larger sample of older adults, resting-state variability in widespread gray matter areas (including primary motor, frontal, cingulate, precuneus, occipital, and temporal regions) was positively associated with factor estimates of episodic memory and fluid intelligence but negatively associated with a vocabulary factor (Burzynska et al., 2015). These resting-state findings suggest that behavioral relationships with BOLD variability might reflect relatively stable individual differences beyond associations with in-scanner task performance.

Although these studies suggest a clear behavioral sensitivity of BOLD variability in resting-state and task-driven fMRI, the precise mechanisms underlying these behavioral relationships remain uncertain. One proposal is that increased BOLD variability might emerge in a neural system that is optimized for environmental uncertainty (Garrett, Samanez-Larkin, et al., 2013). Specifically, the presence of variability in neural responses might allow neural populations to approach Bayesian optimality by representing probabilistic distributions of possible responses (Ma, Beck, Latham, & Pouget, 2006). Such a system might avoid overly deterministic responses, thus affording flexible processing of unpredictable stimuli. Alternatively, BOLD variability might reflect ongoing exploration of potential network configurations or activation states (Deco, Jirsa, & McIntosh, 2011). This mechanism would similarly predict enhanced processing of unexpected inputs as well as more flexible responses. Support for these interpretations comes from observations that BOLD variability parametrically increases as a function of task demands. Specifically, previous studies have shown that variability is (i) greater in task-driven, compared to resting-state, estimates (Garrett, Kovacevic, McIntosh, & Grady, 2013); (ii) greater during tasks requiring responses to changing external stimuli (e.g., vowel judgment, visuomotor responses) versus tasks based on fixed internal representations (e.g., trait judgments; Grady & Garrett, 2018); and (iii) modulated by difficulty in a perceptual face-matching task (Garrett, McIntosh, & Grady, 2014). However, there are also conflicting earlier reports that variability and spontaneous activity might be reduced during task performance as compared to resting state (He, 2011, 2013; Bianciardi et al., 2009; Fransson, 2006), and so the consistency of these effects remains unclear. Moreover, within-participant modulations in BOLD variability across task states have been shown to be less pronounced in older adults and in low task performers (Grady & Garrett, 2018; Garrett et al., 2014; Garrett, Kovacevic, et al., 2013). Hence, the capacity of the system to modulate BOLD variability in accordance with task demands may reflect the integrity of the neural signal related to task performance.

Alternatively, BOLD variability may also relate to functional connectivity or network organization. Specifically, simulation studies suggest that low-frequency BOLD fluctuations might be the outcome of spontaneous activity within a differentially connected network of nodes (Honey, Kötter, Breakspear, & Sporns, 2007). Under this framework, disruptions in the network structure might produce reductions in both the amplitude of these fluctuations (reduced BOLD variability) and the magnitude of the correlations among the fluctuations (reduced functional connectivity). Hence, structural changes in the brain might simultaneously produce differences in both variability and functional connectivity, suggesting that these two measures might be tightly linked, rather than capturing distinct signals. Indeed, at least one study has provided initial evidence for potential links between BOLD variability and functional connectivity, demonstrating that greater BOLD variability within functional networks is associated with stronger functional integration (as defined as lower dimensionality) within those networks (Garrett, Epp, Perry, & Lindenberger, 2018). Under this view, BOLD variability could be related to cognition to the extent that it captures spontaneous activity constrained by a well-connected network structure, rather than capturing ongoing processing within the network. This interpretation might predict that BOLD variability should be related to estimates of structural integrity and connectivity and, moreover, that estimates of variability and their behavioral relationships should be highly consistent within individuals, regardless of changes in states or task contexts, similar to demonstrations of within-individual stability in functional connectivity estimates (Gratton et al., 2018). Other studies have demonstrated relationships between BOLD variability and structural estimates, including hippocampal volume (Good et al., 2020, Millar, Ances, et al., 2020, Zhang et al., 2020) and white matter integrity (Burzynska et al., 2015). Indeed, one study has reported strong correlations between resting-state and task-driven estimates of BOLD variability (Grady & Garrett, 2018); however, these relationships were demonstrated in relatively small samples of 15 older and 20 younger adults. Furthermore, estimates of BOLD variability show fair test–retest reliability over 3-year intervals, at levels comparable to or greater than estimates of functional connectivity (Millar, Petersen, et al., 2020).

Finally, it has also been suggested that resting-state BOLD variability might primarily reflect cardiovascular and/or neurovascular factors, especially in the context of age differences. This suggestion is supported by recent evidence that age-related differences in resting-state BOLD variability are eliminated after correcting for measures of cardiovascular health (CVH; i.e., pulse, heart rate variability, blood pressure, white matter hyperintensities [WMHs], and body mass index [BMI]) and cerebral blood flow (Tsvetanov et al., 2019). However, it is worth noting that there is also evidence that the age relationships with BOLD variability remain after correcting for cardiovascular (Tsvetanov et al., 2015) or neurovascular (Garrett, Lindenberger, Hoge, & Gauthier, 2017) factors alone. In light of these age-related

results, it is possible that cardiovascular factors might also contribute to behavioral relationships with BOLD variability, which would question the above theoretical interpretations of BOLD variability and task performance. Moreover, there is growing interest in potential vascular influences on age-related cognitive decline (for a review, see Abdelkarim et al., 2019; Wåhlin & Nyberg, 2019; O'Brien et al., 2003). Indeed, one recent report demonstrated that relationships between resting-state BOLD variability and a global cognitive composite were eliminated after correcting for similar CVH measures (Millar, Petersen, et al., 2020). However, these relationships have not been examined within specific cognitive domains, so it is unclear whether potential cardiovascular factors may be sensitive to domain-general or domain-specific processing. Furthermore, although multiple studies have considered the influence of cardiovascular factors in estimates of resting-state BOLD variability (Millar, Petersen, et al., 2020; Tsvetanov et al., 2015, 2019; Garrett et al., 2017), we are aware of only one study that has examined these factors in a task-driven context (Garrett et al., 2015).

Some insight into factors underlying behavioral relationships with BOLD variability might be gained by comparing behavioral relationships with variability across resting-state versus task-driven sessions. Although, as discussed above, behavioral relationships have been demonstrated with both resting-state and task-driven variability, no studies have directly compared these relationships. It is possible that these two measures might capture distinct sources of BOLD signal variance and, hence, might offer differential sensitivity to behavioral measures taken inside or outside the scanner. For instance, task-driven BOLD variability might capture unique behaviorally relevant neural processing elicited by the task, which is not present during resting state. In contrast, resting-state BOLD variability captures only spontaneous fluctuations in the BOLD signal, which as mentioned above, may be in part sensitive to cardiovascular sources of variance or network organization. Hence, one might predict that task-driven BOLD variability should be more sensitive than resting-state variability to behavioral measures—even those obtained outside the scanner—and that behavioral relationships with resting-state BOLD variability should be more sensitive to cardiovascular factors. Alternatively, to the extent that BOLD variability reflects underlying network organization, one might expect to see consistency in these estimates and their relationships with behavior across resting-state and task-driven contexts.

In this study, we examined relationships between BOLD variability and cognition, using a large, well-characterized sample of cognitively normal middle-aged to older adults. We obtained composite measures of global cognition, episodic memory, and attentional control, using standard neuropsychological tests and well-established attentional control tasks. Furthermore, we compared relationships of these cognitive composites, as well as in-scanner task performance, to estimates of BOLD variability derived from both resting-state and task-driven fMRI scans. Hence, we are able to evaluate whether behavioral relationships with BOLD variability reflect stable individual differences and whether they are differentially sensitive to spontaneous versus task-evoked sources of variance in the BOLD signal. In addition, we examined the contribution of cardiovascular factors to behavioral relationships with BOLD variability by correcting for measures of CVH, including pulse, blood pressure, BMI, and WMH, and also carefully correcting for motion and global signal artifacts in BOLD variability (see Millar, Petersen, et al., 2020). Finally, in contrast to previous studies, which most often have used a voxel-based or partial least squares approach, we applied a network-based machine learning approach to evaluate whether multivariate patterns in BOLD variability offer predictive accuracy of behavioral measures and, furthermore, whether these relationships follow anatomically meaningful patterns at the level of functional networks (see Millar, Petersen, et al., 2020). Specifically, if BOLD variability reflects an important property of neural processing or network organization, we should expect these relationships to exhibit meaningful anatomical patterns at the network level, especially in those networks most relevant to task performance.

METHODS

Participants

As described previously (Millar, Petersen, et al., 2020), a sample of 190 older adult participants were selected from a larger set of participants enrolled in the Adult Children Study (ACS) and the Healthy Aging and Senile Dementia (HASD) cohorts at the Charles and Joanne Knight Alzheimer Disease Research Center at Washington University in St. Louis. The sample was selected on the basis of having a minimum value of usable resting-state fMRI data (see below); cognitive normality, as carefully assessed by trained clinicians using the Clinical Dementia Rating (Morris, 1993); absence of severe psychiatric conditions; low mean head motion (framewise displacement [FD] < 0.20 mm; see Millar, Petersen, et al., 2020); availability of four estimates of CVH (see below); and availability of at least one cognitive composite measure (see below). One participant was also excluded as a potential outlier (>4 *SD*s from the sample mean), based on average BOLD *SD* across all 298 regions of interest (ROIs; see Calculation of BOLD Variability section).

A subset of 72 participants from the same ACS cohort also completed a task-driven fMRI session, as previously described (Gordon et al., 2015). This subset was selected using the same criteria as the resting-state sample, as well as additional criteria including native English speaker status and minimum performance on in-scanner behavioral tasks (see below). One participant was also excluded as a potential outlier (>4 *SD*s from the sample mean), based on average BOLD *SD* across all ROIs. Table 1 provides a descriptive summary of both resting-state and task-driven fMRI samples. Histograms displaying the distribution of the critical variables are provided in Figure 1. As shown in Table 1, the two samples were well matched in demographic variables, including age, sex, education, and race (ps $> .40$, effect sizes < 0.12). All procedures

Table 1. Demographic and Summary Measures of the Samples

		Resting-State fMRI Sample			*Task-Driven fMRI Sample*					
	Measure (Units)	*N*	*Mean (SD)*	*Range*	*N*	*Mean (SD)*	*Range*	*t*	*p*	*Cohen's d*
Demographic	Age (years)	190	65.05 (8.39)	46–88	72	64.1 (7.56)	49–79	0.84	.40	0.12
	Sex (*n*; female/male)	190	116 / 74	NA	72	47 / 25	NA	0.40[a]	.53[a]	0.04[b]
	Education (years)	178	16.1 (2.42)	12–20	72	16.03 (3.07)	12–20	0.20	.84	0.03
	Race (*n*; White/Black/Asian)	175	167 / 1 / 1	NA	71	69 / 1 / 1	NA	0.81[a]	.67[a]	0.05[b]
	Mean head motion (mm; FD)	190	0.13 (0.03)	0.06–0.2	72	0.14 (0.03)	0.07–0.2	**−2.28**	**.02**	**−0.32**
Psychometric	MMSE (score)	156	29.29 (1.01)	26–30	63	29.43 (0.78)	27–30	−0.94	.35	−0.14
	FCSR: Free Recall (score)	185	32.19 (5.12)	18–46	71	33 (5.93)	21–48	−1.09	.28	−0.15
	WMS Associate Learning (score)	97	14.65 (3.79)	0–21	17	15.74 (3.58)	7–21	−1.09	.28	−0.29
	WMS-R Logical Memory Delayed Recall (score)	97	12.92 (3.95)	5–21	18	13.61 (4.45)	6–21	−0.67	.50	−0.17
	WMS-III Logical Memory Delayed Recall (score)	69	26.94 (7.29)	4–42	45	27.49 (5.4)	12–38	−0.43	.67	−0.08
	Animal Naming (score)	185	22.72 (5.75)	9–41	71	23.44 (5.83)	12–39	−0.88	.38	−0.12
	Trail Making A (score)	185	29.11 (10.64)	12–75	71	27.2 (9.6)	13–57	1.32	.19	0.19
	Trail Making B (score)	184	71.51 (29.82)	28–210	71	60.61 (19.98)	28–139	**2.84**	**.005**	**0.40**
Cardiovascular	Pulse (BPM)	190	68.02 (10.38)	41–108	72	67.67 (10.25)	44–96	0.25	.81	0.03
	Systolic blood pressure (mmHg)	190	124.55 (15.66)	88–168	72	122.94 (14.26)	88–160	0.76	.45	0.11
	BMI (kg/m^2)	190	26.43 (4.43)	17–41	72	26.42 (4.59)	17–40	0.02	.99	0.002
	WMH volume (mm^3)	190	10760.25 (11530.16)	48–61263	72	7848.07 (8312.75)	651–37890	**1.96**	**.05**	**0.27**

MMSE = Mini-Mental State Examination; BPM = beats per minute. **Bold** values reflect statistically significant group differences.

[a] *T* and *p* values are from independent-samples *t* tests between the resting-state and task-driven samples, except for categorical variables tested by chi-square test (χ^2), as noted by Footnote a.

[b] Effect sizes are reported as Cohen's *d*, except for categorical variables reported as Cramer's *V*, as noted by Footnote b.

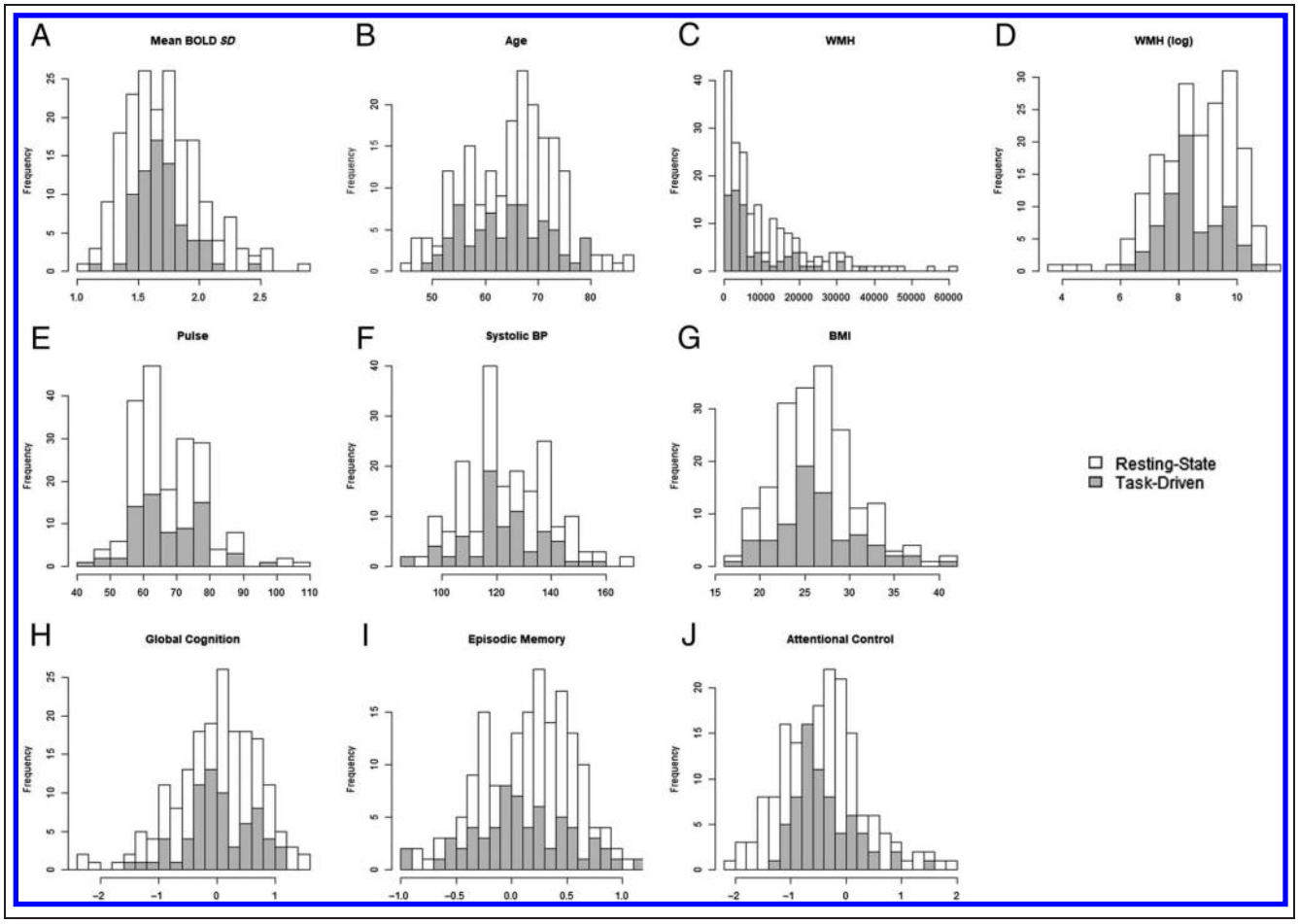

Figure 1. Histograms of critical measures used in the present analyses including mean BOLD *SD* across all ROIs (A), age (B), CVH measures (C–G), and cognitive composite scores (H–J). Distributions of each variable are presented separately for the resting-state (white) and task-driven (gray) samples.

were approved by the Human Research Protection Office at Washington University in St. Louis. All participants provided informed consent before all procedures.

Psychometric Composites of Global Cognition and Episodic Memory Tasks

Each participant completed a 2-hr battery of neuropsychological tests. To investigate relationships between BOLD variability, episodic memory, and global cognitive function, we examined performance on a subset of tasks across multiple cognitive domains. Measures of episodic memory included the Free and Cued Selective Reminding Test (FCSR) free recall score (Grober, Buschke, Crystal, Bang, & Dresner, 1988), the Associate Learning subtest from the Wechsler Memory Scale (Wechsler & Stone, 1973), and delayed recall scores from two versions of the Logical Memory test (Wechsler Memory Scale-Revised: Wechsler, 1987; Wechsler Adult Intelligence Scale [WAIS-III], Wechsler, 1997), which differed across the ACS and HASD cohorts. An episodic memory composite was calculated as the average of standardized FCSR free recall, associate learning, and logical memory delayed recall, as this composite has been used as a sensitive individual difference measure (Aschenbrenner et al., 2015). As shown in Table 2, we observed strong positive relationships between all measures in the episodic memory composite (Pearson's *r*s from .48 to .75). Because of missing data in several of the behavioral tasks, we allowed for up to one missing value in the calculation of each cognitive composite.

We also examined a global cognitive composite, which included measures of semantic fluency (Animal Naming: Goodglass & Kaplan, 1983), processing speed (Trail Making A: Armitage, 1946), and executive function (Trail Making B: Armitage, 1946) as well as FCSR free recall. The global cognitive composite was calculated as the average of standardized FCSR free recall, Animal Naming, and reverse-scored Trail Making A and B and has also been used as a sensitive individual difference measure (Aschenbrenner, Gordon, Benzinger, Morris, & Hassenstab, 2018). As shown in Table 2, we observed moderate relationships in the expected directions between all measures in the global composite (absolute *r*s from .15 to .57).

Attentional Control Composite Tasks

In addition to the neuropsychological test batteries, participants also completed a battery of computerized attentional

Table 2. Correlations among Neuropsychological and Cognitive Test Measures in the Resting-State fMRI Sample

	FCSR: Free Recall	*Associate Learning*	*Logical Memory*	*Animal Naming*	*Trails A*	*Trails B*	*Stroop Effect*	*Simon Effect*	*Global Switch*
FCSR: Free Recall		**.75*** **	**.72*** **	**.22†**	**−.32****	**−.16**	−.28*	−.06	−.28*
Associate Learning	**.53*** **		**.63****	.21	−.69***	−.51*	−.4	−.14	−.54*
Logical Memory	**.48*** **	**.54*** **		.11	−.35	−.18	−.17	−.28	−.11
Animal Naming	**.41*** **	.24**	.37***		**−.15**	**−.17**	−.22	.12	−.16
Trails A	**−.25*** **	−.21**	−.05	**−.29*** **		**.5*** **	.3*	.21†	.11
Trails B	**−.28*** **	−.28***	−.2**	**−.3*** **	**.57*** **		.31*	.05	.28*
Stroop effect	−.26**	−.23†	−.24*	−.09	.33***	.37***		**.27***	**.39****
Simon effect	−.17**	−.12	−.08	−.18**	.45***	.23***	**.27****		**.01**
Global switch	−.33***	−.24**	−.24**	−.36***	.35***	.32***	**.19***	**.21*** **	

Correlations in the resting-state sample are presented in the lower triangle. Correlations in the task-driven sample are presented in the upper triangle. Bold values reflect correlations between measures assigned to a common a priori cognitive composite.

† $p < .10$.

* $p < .05$.

** $p < .01$.

*** $p < .001$.

control tasks. Participants completed a Stroop color-naming task (Spieler, Balota, & Faust, 1996; Stroop, 1935), a Simon spatial interference task (Castel, Balota, Hutchison, Logan, & Yap, 2007; Simon, 1969), and a consonant–vowel/odd–even (CVOE) task-switching task (Huff, Balota, Minear, Aschenbrenner, & Duchek, 2015).

Briefly, in the Stroop task, participants viewed 36 congruent color words ("blue," "green," "red," or "yellow" presented in the corresponding color), 36 incongruent color words (the same four color words presented in a nonmatching color), and 32 neutral words ("poor," "deep," "bad," or "legal" presented in one of the four colors). Participants were instructed to vocally name the color of each word into a microphone. Accuracy of each trial was coded by an experimenter as correct, incorrect, or microphone error.

In the Simon task, participants viewed 40 congruent horizontal arrows (facing left or right and appearing on the corresponding side of the screen), 40 incongruent arrows (appearing on the opposite side of the screen as the direction of the arrow), and 40 neutral arrows (appearing in the center of the screen). Participants were instructed to manually report the direction of the arrow (left or right) by button press.

The CVOE task consisted of two task-pure blocks and a task-switching block. During each pure block, participants viewed 48 letter–number pairs (e.g., "D 06") and were instructed to manually classify either the letter (consonant or vowel) or the number (odd or even) by button press. During the switch block, participants were cued to make letter or number classifications in alternating runs of two trials for each classification type, resulting in 30 switch trials (in which participants switched from one dimension to the other) and 30 nonswitch trials (in which participants repeated the same response dimension).

In each task, performance was assessed using the difference score of RTs between two conditions of interest. In all tasks, we examined only RTs from accurate trials. To limit the influence of extreme outliers, we excluded individual trials with RTs less than 200 msec or greater than 3 *SD*s above or below the individual participant's mean RT on each task. The Stroop and Simon effects (difference between incongruent and congruent trials) are established indices of selective attention or interference, whereas the global switch effect (difference between nonswitch trials in CVOE switch blocks and pure block trials) is thought to reflect the cost of maintaining multiple task sets. Hence, we calculated an attentional control composite as the average of the standardized Stroop effect, Simon effect, and global CVOE switch cost measures. We have used a similar composite of estimates from these same tasks as a sensitive individual difference marker (Aschenbrenner et al., 2015). As shown in Table 2, we observed moderate, significant correlations between most of the attentional control difference scores (*r*s from .19 to .39), except for the relationship between Simon effect and global CVOE switch cost in the smaller task-driven fMRI sample.[1]

It is possible that individual differences in processing speed might contribute to RT differences in the attentional composite tasks. Hence, we used a standard estimate of

processing speed (performance on Trails A) as a covariate to control for the influence of processing speed on RT difference scores (see Wolf et al., 2014). We present relationships with attentional control before and after residualizing the composite for Trails A performance to examine whether relationships with attentional control are observed after correcting for processing speed.

CVH Measures

On the basis of recent demonstrations that BOLD variability may be sensitive to individual differences in CVH (Millar, Petersen, et al., 2020; Tsvetanov et al., 2019), we examined available measures of CVH, including resting pulse, systolic blood pressure, BMI, and WMH lesion volume. WMH volumes were assessed with a fluid-attenuated inversion recovery sequence, after segmentation using the Lesion Segmentation Tool (Schmidt et al., 2012) for SPM8. We used estimates of pulse, systolic blood pressure, BMI, and WMH as CVH covariates in the analyses where indicated below.[2]

Structural, Resting-State, and Task-Driven Scanning Protocols

MRI data were obtained using two separate Siemens Trio 3-T scanners with a standard 12-channel head coil. To examine the possibility that behavioral relationships with resting-state BOLD variability might be confounded by differences in the scanners, we also tested the results with each composite after controlling for scanner as a factor of noninterest. The observed relationships were consistent after controlling for the scanner. Structural and functional scans were acquired using methods described previously (Millar, Petersen, et al., 2020; Brier et al., 2012). Structural scans were acquired with a sagittal T1-weighted magnetization prepared rapid gradient echo sequence (repetition time [TR] = 2400 msec, echo time [TE] = 3.16 msec, flip angle = 8°, field of view = 256 mm, 1-mm isotropic voxels) as well as an oblique T2-weighted fast spin echo sequence (TR = 3200 msec, TE = 455 msec, 256 × 256 acquisition matrix, 1-mm isotropic voxels).

Resting-state functional scans were acquired with an interleaved whole-brain echo-planar imaging (EPI) sequence (TR = 2200 msec, TE = 27 msec, flip angle = 90°, field of view = 256 mm, 4-mm isotropic voxels). Participants completed two consecutive runs of resting-state functional imaging (6 min, 164 volumes each), during which they were instructed to stay awake and fixate on a visual crosshair.

As described previously (Gordon et al., 2015), task-driven functional scans were acquired in a separate session with an interleaved whole-brain EPI sequence (TR = 2000 msec, TE = 25 msec, flip angle = 90°, field of view = 256 mm, 4-mm isotropic voxels). Participants completed two runs of an animacy judgment task (10 min 6 sec, 303 volumes each), followed by two runs of a Stroop color-naming task (9 min 50 sec, 295 volumes each).

Briefly, during each task run, participants alternated between five blocks of rest (30 sec each) and four blocks of task performance (114 sec each for animacy; 110 sec for Stroop). During rest intervals, participants fixated on a visual crosshair. During each animacy task block, participants viewed a randomly intermixed sequence of 24 words (12 living and 12 nonliving), which were balanced for length, frequency, and orthographic neighborhood. On each trial, participants were instructed to manually report via a keypress whether the word represented a living or nonliving thing. During each Stroop task block, participants viewed a randomly intermixed sequence of 12 congruent color words (e.g., "red" in red), 12 incongruent color words (e.g., "blue" in red), and 12 neutral words (e.g., "deep" in red). On each trial, participants were instructed to manually report via a keypress whether the word was presented in a red or blue color. In both tasks, each word appeared for 1 sec, followed by a jittered intertrial interval of 1, 3, 5, or 9 sec. Participants completed practice trials of both tasks before entering the scanner.

Functional Preprocessing

Because we have demonstrated that estimates of BOLD variability are influenced by differences in head motion (Millar, Petersen, et al., 2020), we conservatively controlled for artifact-related influences in the current data set using global signal regression (GSR), censoring of high-motion frames, and exclusion of individuals with high mean head motion. Initial preprocessing for both resting-state and task-driven fMRI data followed conventional methods, as described previously (Millar, Ances, et al., 2020; Brier et al., 2012; Shulman et al., 2010). Briefly, these steps included frame alignment, debanding, rigid body transformation, bias field correction, and mode 1000 normalization. Transformation to an age-appropriate atlas template in 711-2B space was performed using a composition of affine transforms connecting the functional volumes with the T2-weighted and magnetization prepared rapid gradient echo images. Head movement correction was included in a single resampling that generated a volumetric time series in isotropic 3-mm atlas space.

As described previously (Millar, Petersen, et al., 2020; Fox, Zhang, Snyder, & Raichle, 2009), additional processing was performed to allow for nuisance variable regression. First, masks of whole brain, gray matter, white matter, and CSF were generated from T1 images in FreeSurfer 5.3 (Fischl, 2012). Second, two indices of framewise motion were calculated across the BOLD time series, including FD (Power, Barnes, Snyder, Schlaggar, & Petersen, 2012) and derivative of root mean squared variance over voxels (DVARS) root mean squared. Third, BOLD data were subjected to a temporal band-pass filter ($0.005\ \text{Hz} < f < 0.1\ \text{Hz}$). Fourth, BOLD data were subjected to nuisance variable regression, including six motion parameters, time series from the whole brain (global signal), CSF, ventricle, and white matter masks, as well as the derivatives of these

signals. Task-driven fMRI data were subjected to additional nuisance regressors of the task block design within runs (Fair et al., 2007). Finally, BOLD data were spatially blurred (6-mm full width at half maximum).

Preprocessed BOLD data were subjected to framewise censoring based on motion estimates. Specifically, volumes were censored if FD exceeded 0.2 mm or if DVARS exceeded 2.5 *SD*s from the participant's mean. Motion-related differences in the number of censored frames might confound the magnitude and/or reliability of BOLD variability estimates. Moreover, differences in the number of usable frames may bias BOLD variability estimates between the resting-state and task-driven scans, which were of different lengths. Thus, we analyzed BOLD variability during resting-state within a subset of 200 randomly selected usable frames from either resting-state run for each participant. Participants with fewer than 200 usable frames were excluded. Similarly, we analyzed task-driven BOLD variability within a subset of 200 randomly selected usable task block frames for each participant (100 from animacy task blocks, 100 from Stroop task blocks).[3] Finally, we analyzed BOLD variability during fixation blocks between task blocks within a subset of 100 randomly selected usable frames. To control for mean differences across blocks, we subtracted the voxelwise block means from the time series data before concatenating task or fixation blocks (Garrett et al., 2010). We also examined variability estimates from each task separately (using 200 randomly selected frames per task) but found evidence of multivariate relationships between BOLD variability and head motion in both tasks even after applying GSR and framewise censoring (R^2s from SVR models' prediction head motion = .162, .117; ps ≤ .003; cf. Millar, Petersen, et al., 2020).[4] Hence, to minimize the potential confounding influence of motion, we focus on variability from the concatenated task blocks including both animacy and Stroop performance, in which the multivariate sensitivity was eliminated (R^2 = .016, p = .276). BOLD variability estimates in 298 ROIs (see Calculation of BOLD Variability section) during Stroop and animacy tasks were highly correlated (average r = .78, range = .53–.95).

Calculation of BOLD Variability

As described previously (Millar, Petersen, et al., 2020), final BOLD time series data were averaged across voxels within 298 ROIs from an expanded version of a previously defined atlas (Seitzman et al., 2020; Power et al., 2011), including two hundred forty-three 10-mm cortical spheres, twenty-eight 8-mm subcortical spheres, and twenty-seven 8-mm spheres in the cerebellum (see Seitzman et al., 2020, for a figure). Importantly, each ROI was assigned to 1 of 13 networks, including somatomotor (SM), lateral SM (SML), cingulo-opercular (CO), auditory (AUD), default mode (DMN), parietal memory (PMN), visual (VIS), frontoparietal (FPN), salience (SAL), subcortical (SUB), ventral attention (VAN), dorsal attention (DAN), and cerebellum (CER). In each ROI, we calculated the *SD* of the BOLD signal over the 200 selected usable resting-state frames, 200 usable task-driven frames, or 100 fixation frames in the residualized time series data after applying nuisance regression and framewise censoring. These *SD* values served as our regional estimates of BOLD variability.[5]

Support Vector Regression

Support vector regression (SVR) analyses were conducted using the e1071 package in R (Meyer et al., 2017). Briefly, SVR is a supervised machine learning technique in which a model is trained to identify multivariate relationships between a set of features (i.e., resting-state or task-driven BOLD *SD*s in the 298 ROIs) and a continuous label (e.g., composites of global cognition, episodic memory, or attentional control). We performed epsilon-insensitive SVR, as described previously (Millar, Petersen, et al., 2020; Nielsen, Greene, et al., 2019; Dosenbach et al., 2010). Briefly, in each training fold, a regression line is fit in multivariate space between the feature set values and the label values. A tube of width epsilon is defined around the regression line. Data points outside this tube are penalized, whereas points inside the tube are not. The penalty factor C determines the trade-off between training error and model complexity. All SVR analyses were performed with $\varepsilon = 0.00001$ and C = infinity, based on previous reports predicting age from functional connectivity (Nielsen, Greene, et al., 2019; Dosenbach et al., 2010) and BOLD variability (Millar, Petersen, et al., 2020).

Importantly, the SVR model is trained on a subset of cases (the training set), allowing for the assessment of model prediction in an unseen set of cases (the testing set). Specifically, we evaluated predictive accuracy using 10-fold cross-validation. For each of the 10 folds, a nonoverlapping set of 10% of the sample served as the testing set. The remaining 90% served as the training set. Thus, across the 10 folds, the SVR model predicted a label value for each participant. We quantified predictive accuracy as R^2 between the model-predicted and true label values for each participant. We tested the predictive accuracy of SVR models trained on the full feature set of BOLD *SD* values from all 298 ROIs. Specifically, we tested the performance of these models to predict cognitive composites and measures of in-scanner behavioral performance as labels of interest. Thus, the SVR approach evaluates the predictive sensitivity of BOLD *SD* for domain-specific cognitive estimates in untrained observations, which has not been assessed in previous studies of BOLD variability.

Assessment of Network Specificity of Relationships

Network specificity of relationships with BOLD *SD* was assessed in two ways. First, univariate regional correlations were calculated between the measure of interest and BOLD *SD* within each of the 298 ROIs. Significance of network-level relationships was tested using a bootstrap approach with 10,000 samples by resampling the data set with replacement. In each bootstrap sample, we calculated the

correlation with the measure of interest in each ROI and then averaged the correlation values across ROIs within each network. Across bootstrap samples, we then calculated the empirical 95% confidence interval for each network-level correlation.

Second, we assessed the multivariate predictive accuracy of networks using feature selection. Specifically, SVR models predicted a measure of interest from a limited feature set of regions restricted to a single network. Because larger networks should perform better simply because of a greater number of features, which might capture a related signal by chance, we compared SVR performance for network-specific feature sets to a bootstrapped distribution of 10,000 randomly selected feature sets (i.e., random regions from any network), which were matched in the number of features. Hence, this distribution is an appropriate null model to test whether signals are localized to specific networks or instead broadly distributed throughout the brain (Nielsen, Barch, Petersen, Schlaggar, & Greene, 2020).

RESULTS

Comparison of Resting-State and Task-Driven BOLD Variability Estimates

To examine BOLD variability in resting-state versus task-driven scans, we first compared estimates of BOLD *SD* within each network as a function of scan type (resting-state vs. task-driven) using a subset of 40 participants who had usable scans of both types collected on the same day. We tested for main effects of scan type and network as well as the Scan × Network interaction using a repeated-measures analysis of variance (ANOVA). Overall, we observed a main effect of scan type ($F = 9.05, p = .005, \eta_p^2 = .19$), such that on average, resting-state BOLD *SD* ($M = 1.79$) was greater than task-driven BOLD *SD* ($M = 1.61$). This main effect was further characterized by a significant Scan × Network interaction ($F = 31.60, p < .001, \eta_p^2 = .44$). As shown in Figure 2A, resting-state BOLD *SD* was significantly greater than task-driven BOLD *SD* in most networks (SM, SML, DMN, PMN, VIS, FPN, SAL, SUB, VAN, and DAN networks; ps ≤ .021, Cohen's ds from 0.38 to 1.38), although task-driven BOLD *SD* was significantly greater in the CER network ($p < .001$, Cohen's $d = 1.19$).

We also compared estimates of BOLD *SD* in each network as a function of block type (fixation vs. animacy vs. Stroop) using a subset of 71 participants who had usable *SD* estimates for each block (100 concatenated usable frames per block type). We tested the main effects and interaction of block type and network, using a repeated-measures ANOVA. We observed a main effect of block type ($F = 72.68, p < .001, \eta_p^2 = .51$). Post hoc comparisons revealed that, on average, BOLD *SD* during fixation ($M = 1.81$) was significantly greater than BOLD *SD* during the animacy task ($M = 1.62, t = 9.17, p < .001$, Cohen's $d = 1.09$) and also greater than BOLD *SD* during Stroop ($M = 1.62, t = 11.03, p < .001$, Cohen's $d = 1.31$). This main effect was also characterized by a significant Block × Network interaction ($F = 9.31, p < .001, \eta_p^2 = .12$). As shown in Figure 2B, BOLD *SD* in each network was significantly greater during fixation than during the animacy blocks (ps < .001, Cohen's ds from 0.69 to 1.40) or during the Stroop blocks (ps < .001, Cohen's ds from 0.68 to 1.73). In contrast, differences in network estimates of BOLD *SD* between the animacy and Stroop blocks were smaller and in no consistent direction. Specifically, variability was significantly greater during animacy than

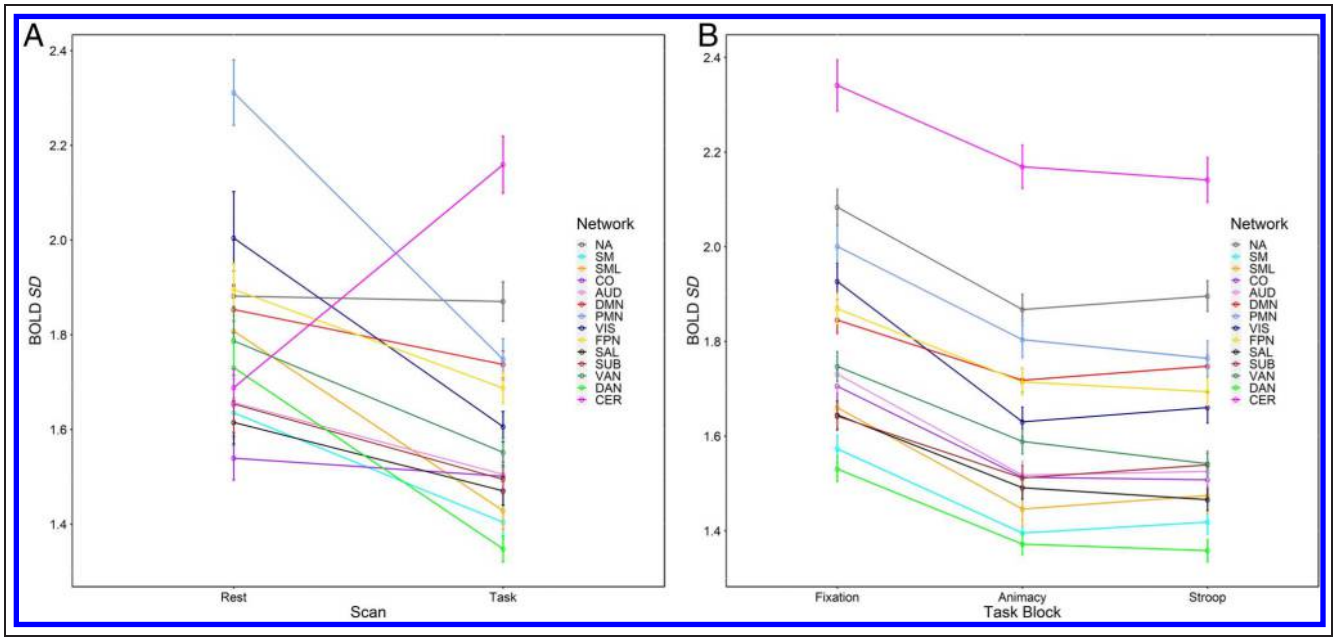

Figure 2. Network-level BOLD *SD* as a function of scan type (A; resting-state vs. task-driven) and block type within the task-driven scan (B; fixation vs. animacy vs. Stroop). Error bars display *SEM*.

Stroop in the VAN ($p = .02$, Cohen's $d = 0.28$), but other networks were at most marginally different between tasks (ps ≥ .08, Cohen's ds from 0.04 to 0.21).

In addition, we assessed the consistency of BOLD variability estimates across scans by calculating the regional correlations between resting-state and task-driven BOLD variability within the same subset of participants. The correlations between resting-state and task-driven BOLD *SD* estimates were surprisingly low (average $r = .30$, range = −.19 to .80). Of course, this low correlation could be because of low reliability of the task-driven or resting-state BOLD *SD* estimates. As noted, BOLD variability estimates during Stroop and animacy tasks were highly correlated with each other (average $r = .78$, range = .53–.95). Hence, it appears that the task-driven BOLD *SD* is stable, at least between runs within one session. In addition, as reported in an overlapping subset of the current sample by Millar and colleagues (2020), the test–retest reliabilities of the resting-state BOLD *SD* estimates are quite stable, as reflected by moderate correlations over a 3-year longitudinal follow-up (average $r = .46$, range = .18–.71) and indeed were comparable to intranetwork connectivity estimates in this same sample (average $r = .45$, range = .30–.60).

Relationships with Cognitive Composite Measures

Global Cognition

As shown in Table 3, SVR models were able to successfully predict global cognition scores from the full feature set of resting-state BOLD *SD* using all 298 ROIs ($R^2 = .045$, $p = .004$). We evaluated the multivariate relationship between global cognition and resting-state BOLD *SD* in terms of specific networks using network-driven feature selection. As shown in Figure 3A, BOLD *SD* estimates within the DAN ($R^2 = .014$) and DMN ($R^2 = .011$) were relatively successful in predicting global cognition, compared to other networks. This level of performance might be expected in the DMN, because it includes a large number of individual ROIs and may capture related signal by chance. Hence, we tested the specificity of these network relationships by comparing SVR performance from the DAN and DMN to bootstrapped distributions of 10,000 randomly selected regions of equal set size from any network. SVR performance from the DAN did not outperform the matched bootstrapped distribution (empirical $p = .232$), nor did the DMN (empirical $p = .619$). Indeed, SVR performance from all networks fell within the range expected by randomly selected regions. Hence, the multivariate relationship between BOLD *SD* and global cognition is likely spread throughout networks with little anatomical specificity (Figure 3).

However, global cognition did not relate to BOLD *SD* in the task-driven fMRI sample. As shown in Table 3, SVR models were not able to predict global cognitive scores from task-driven BOLD *SD* ($R^2 = .025$, $p = .188$). Thus, the global cognitive relationships observed during resting-state do not replicate in estimates of task-driven BOLD *SD*.[6]

Episodic Memory

As shown in Table 3, SVR models were not able to predict episodic memory scores from resting-state BOLD *SD* ($R^2 = .007$, $p = .279$). In the task-driven fMRI sample, the slope between true episodic memory composite scores and values predicted by the SVR model was significantly *negative* ($r = -.395$, $R^2 = .156$, $p = .001$; see Table 3), suggesting that the model was not able to accurately predict episodic memory based on estimates of task-driven BOLD *SD*.

Attentional Control

As shown in Table 3, SVR models were able to successfully predict attentional control from resting-state BOLD *SD* using all 298 ROIs ($R^2 = .106$, $p < .001$). We evaluated the multivariate relationship between the attention composite and resting-state BOLD *SD* in terms of specific networks using network-driven feature selection. As shown in Figure 3B, BOLD *SD* estimates within the VIS network ($R^2 = .060$) were relatively successful in predicting the attention composite, compared to other networks, and marginally outperformed a matched bootstrapped distribution (empirical $p = .062$). Hence, the multivariate relationship between BOLD *SD* and attentional control may be particularly strong in the VIS network.

As noted, raw RT difference scores in the attentional control tasks may be influenced by individual differences in processing speed. Hence, we sought to test BOLD *SD* relationships with the attentional control composite after residualizing performance on Trails A to control for processing speed. SVR models were marginally successful in predicting the corrected attentional control scores from resting-state BOLD *SD* ($R^2 = .020$, $p = .067$; see Table 2). Hence, after correcting for processing speed, resting-state BOLD *SD* may still capture a small portion of variance in estimates of attentional control.

Turning now to task-driven BOLD *SD*, we found that the attentional control composite was again related to BOLD *SD*. As shown in Table 3, SVR models were able to successfully predict attentional control from task-driven BOLD *SD* ($R^2 = .135$, $p = .002$). Again, we evaluated the multivariate relationship between attention and task-driven BOLD *SD* in terms of specific networks using network-driven feature selection. As shown in Figure 3C, BOLD *SD* estimates within the CO network ($R^2 = .201$) were particularly successful in predicting attentional control, compared to other networks, and significantly outperformed a matched bootstrapped distribution (empirical $p = .036$). SVR performance from other networks fell within the range expected by randomly selected regions (empirical ps ≥ .222). Hence, the multivariate relationship between task-driven BOLD *SD* and attentional control may be particularly strong in the CO network.

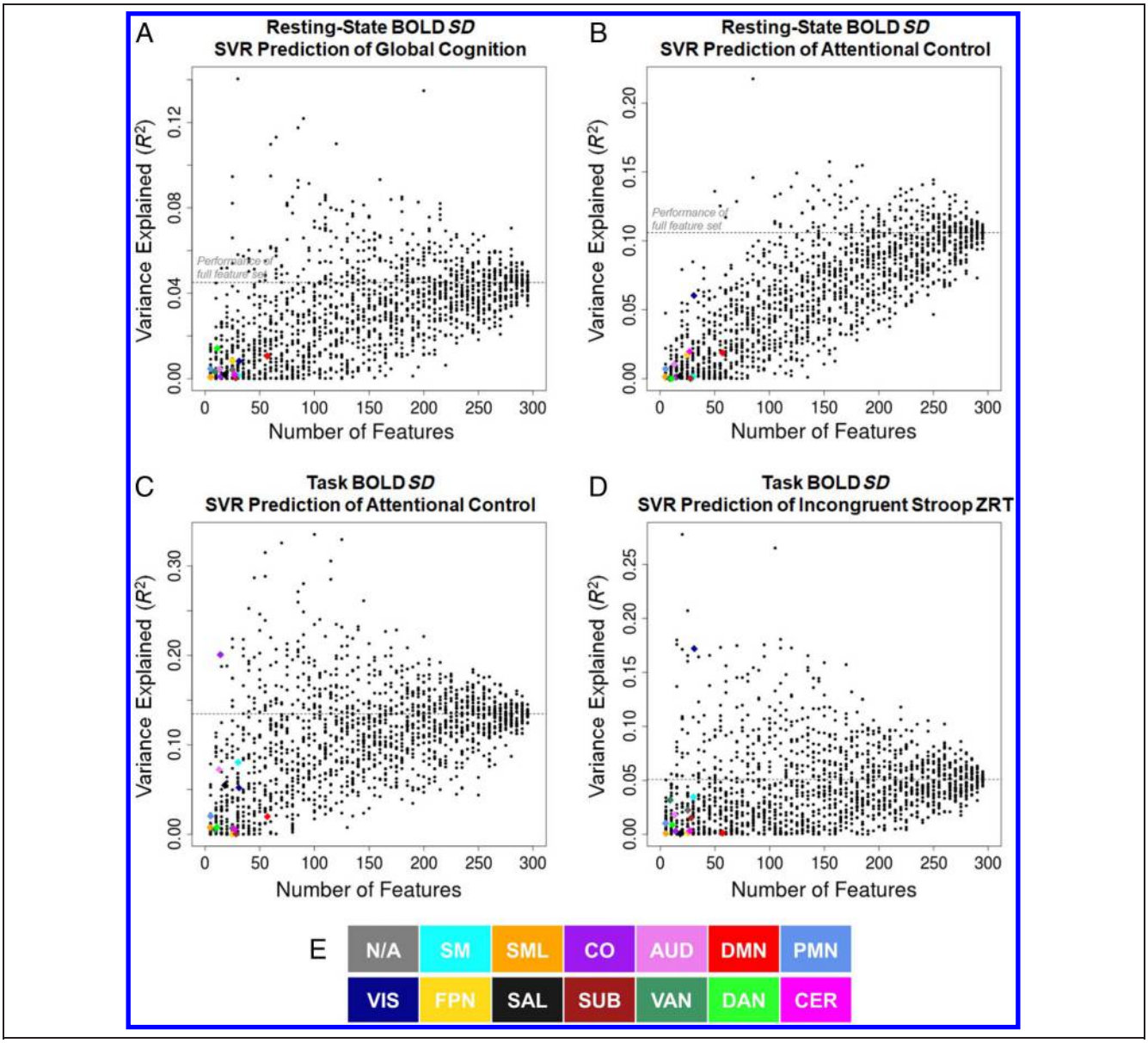

Figure 3. Performance of SVR models predicting global cognition (A), attentional control (B and C), and in-scanner incongruent Stroop ZRT (D) across a range of feature sets (from 5 to 295). Models in A and B use resting-state BOLD *SD* as inputs, whereas models in C and D use task-driven BOLD *SD*. Colored diamonds denote anatomical feature selection schemes, in which features included only ROIs from a specific network. Each network-specific model was compared to 10,000 simulated models using randomly selected feature sets from any functional network. For simplicity, only 25 of the simulated models are plotted for each feature set size (black dots). (E) Color key for network identities.

As shown in Table 3, SVR models were also able to predict attentional control from task-driven BOLD *SD* after correcting for processing speed in estimates residualized for Trails A performance ($R^2 = .141$, $p = .002$). Hence, relationships with attentional control observed in the resting-state estimates were generally consistent in task-driven BOLD *SD*.

Age-related Influences on Cognitive Relationships

Although the observed behavioral relationships with resting-state and task-driven BOLD variability are consistent with previous studies (e.g., Garrett et al., 2011), it is possible that these relationships might be sensitive to age-related variability. As noted, we and others have demonstrated that BOLD variability is associated with age (e.g., Garrett et al., 2010), including within a mostly overlapping sample (see Millar, Petersen, et al., 2020). Moreover, there were indeed significant age relationships with the global ($r = -.42$, $p < .001$) and attentional ($r = .36$, $p < .001$) composite measures. Thus, in the current sample, BOLD variability might only relate to cognition to the extent it is sensitive to age in general. Hence, we sought to test the observed relationships between cognitive composite

scores and residual BOLD *SD* estimates during both resting-state and task-driven runs after controlling for age as a continuous covariate using a regression approach.

As shown in Table 3 and Figure 4 (left column), most relationships between cognitive composites and resting-state BOLD *SD* were eliminated after controlling for age. Specifically, global cognition was not associated with BOLD *SD* in any network (see Figure 4A), nor were SVR models successful in predicting global cognition from corrected resting-state BOLD *SD* estimates ($R^2 < .001$; see Table 3). In addition, episodic memory was not associated with resting-state BOLD *SD* in any network, (see Figure 4C), nor were SVR models successful in predicting episodic memory ($R^2 = .018$; see Table 3).

Turning to the attentional control composite, negative relationships with resting-state BOLD *SD* were eliminated in all networks after correcting for age (see Figure 4E and G). SVR models were unsuccessful in predicting attentional control after correcting for age (R^2s ≤ .002; see Table 3).

In contrast to the resting-state results, correction for age had a much smaller influence on cognitive relationships with task-driven BOLD *SD*. Estimates of task-driven BOLD *SD* were largely unrelated to global cognition (Figure 4B) and episodic memory (Figure 4D) after correcting for age (see Table 3). However, as noted above, minimal relationships were observed with these measures in the uncorrected task-driven BOLD *SD* estimates, and thus, no relationships should be expected in the age-corrected estimates.

Most importantly, as shown in Figure 4F and H, we continued to observe marginal to significant negative relationships between the attentional control composite and task-driven BOLD *SD* after correcting for age. Specifically, greater task-driven BOLD *SD* estimates in several networks (including CO, DMN, PMN, VIS, FPN, SAL, VAN, DAN, and CER) were associated with reduced attentional control costs. In addition, these relationships were consistent even after further correcting for individual differences in processing speed. Furthermore, SVR prediction was still successful for the attention composite both before ($R^2 = .141$, $p = .002$) and after ($R^2 = .139$, $p = .002$) correcting for processing speed (see Table 3). Hence, although cognitive relationships with resting-state BOLD variability may be influenced by age-related variability, relationships with task-driven variability remain after correcting for age and, thus, may be sensitive to distinct sources of variance.

Cardiovascular Influences on Cognitive Relationships

One potential mechanism through which age may influence cognitive relationships with BOLD variability is CVH. Recent studies have demonstrated that age relationships with BOLD variability are attenuated after correcting for individual differences in CVH and/or cerebral blood flow (Millar, Petersen, 2020; Tsvetanov et al., 2019). However, it is unclear whether cardiovascular mechanisms might contribute to domain-specific cognitive relationships with BOLD variability. Hence, we sought to test the observed relationships between cognitive composite scores and residual BOLD *SD* estimates after controlling for cardiovascular factors. As noted above, we used individual estimates of

Table 3. Performance of SVR Models (R^2 Statistic) Predicting Cognitive Composite Measures

Data Set	*Cognitive Composite*	*SVR R^2 (Uncorrected)*	*SVR R^2 (Partial Age)*	*SVR R^2 (Partial CVH)*
Resting-state fMRI	Global	.045**	<.001	.005
	Episodic memory	.007	.018	.021
	Attentional control	.106***	.002	.007
	Attentional control (corrected for Trails A)	.020†	<.001	<.001
Task-driven fMRI	Global	.025	.024	.002
	Episodic memory	*.156*	*.133*	*.178*
	Attentional control	.135**	.141**	.062*
	Attentional control (corrected for Trails A)	.141**	.139**	.093*

Performance is presented for uncorrected models, as well as after statistically controlling for age and CVH variables as covariates in BOLD *SD* estimates. *Italics* denote negative slopes between true and predicted values.

† $p < .10$.

* $p < .05$.

** $p < .01$.

*** $p < .001$.

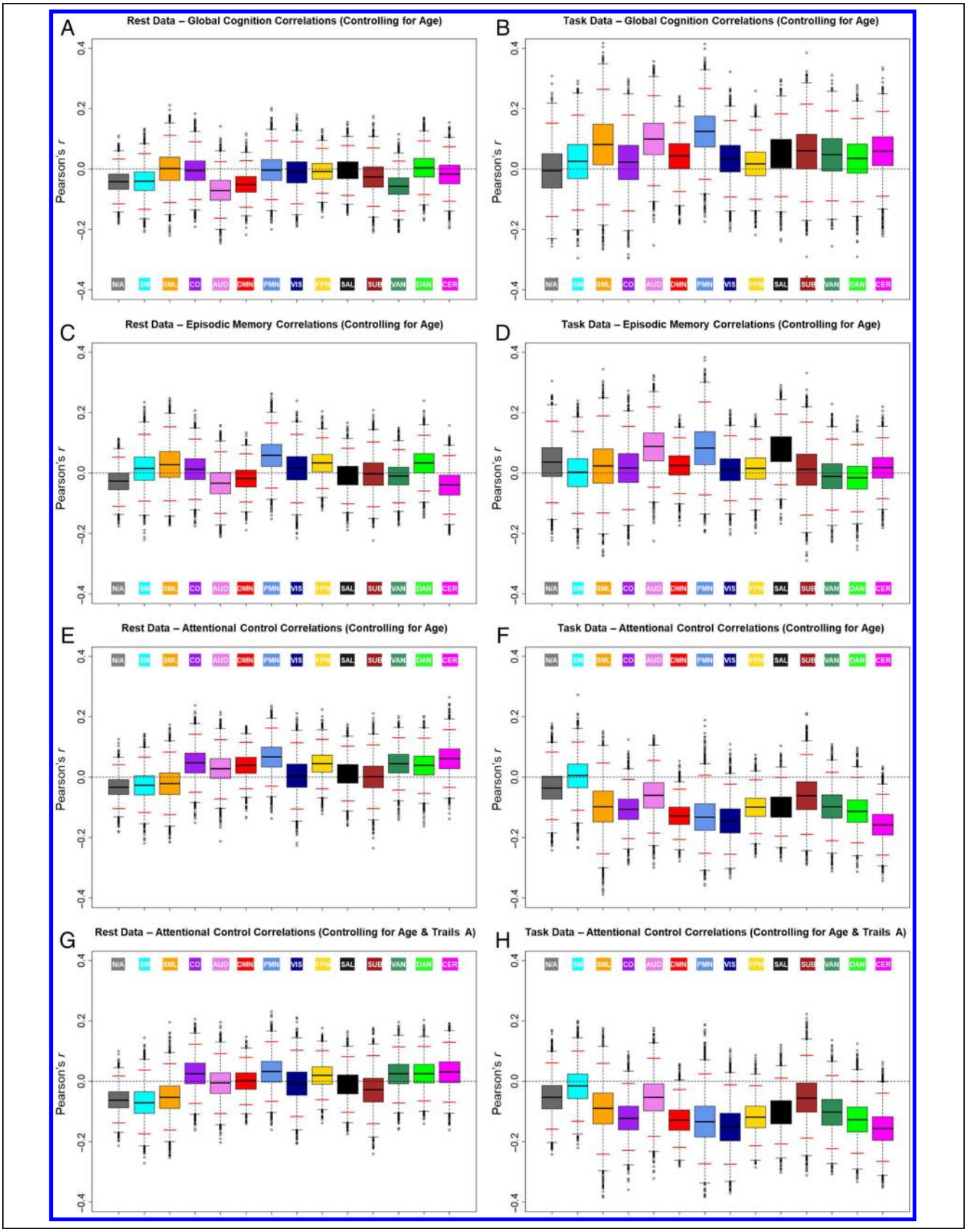

Figure 4. Boxplots of the distribution of bootstrapped distributions of network average Pearson correlations between BOLD *SD* and global cognition (A and B), episodic memory (C and D), attentional control (E and F), and attentional control corrected for Trails A (G and H) after controlling for age. Relationships are shown for both resting-state (left column; A, C, E, and G) and task-driven (right column; B, D, F, and H) fMRI sessions. Distributions in which the 95% confidence interval (red lines) excludes 0 (dotted black line) reflect significant network-level relationships.

pulse, systolic blood pressure, BMI, and WMH as covariates to control for individual differences in CVH.

As shown in Figure 5 (left column) and Table 3, most relationships between cognitive composites and resting-state BOLD *SD* were eliminated after controlling for CVH measures, similar to the effect of controlling for age. Specifically, global cognition was not associated with BOLD *SD* in any network (see Figure 5A), nor were SVR models successful in predicting global cognition from corrected resting-state BOLD *SD* estimates (R^2 = .005; see Table 3), consistent with a previous report from a mostly overlapping sample (Millar, Petersen, et al., 2020). In addition, episodic memory was not associated with resting-state BOLD SD in any network after controlling for CVH (see Figure 5C and D), nor were SVR models successful in predicting episodic memory (R^2 = .021; see Table 3).

Turning to the attentional control composite, negative relationships with resting-state BOLD *SD* were eliminated in all networks after correcting for CVH (see Figure 5E and G). Furthermore, SVR models were unsuccessful in predicting the attention composite after correcting for CVH (R^2s ≤ .007; see Table 3).

Similar to the age corrections, however, correction for CVH had a much smaller influence on cognitive relationships with task-driven BOLD *SD*. Estimates of task-driven BOLD *SD* were largely unrelated to global cognition (Figure 5B) and episodic memory (Figure 5D) after correcting for CVH (see Table 3). However, as noted above, minimal relationships were observed with these measures in the uncorrected task-driven BOLD *SD* estimates, and thus, no relationships should be expected in the cardiovascular-corrected estimates.

Most importantly, as shown in Figure 5F and H, marginal to significant negative relationships between the attentional control composite and task-driven BOLD *SD* were again consistently observed in similar networks after correcting for CVH. Specifically, greater task-driven BOLD *SD* estimates in CO, DMN, PMN, VIS, FPN, SAL, DAN, and CER networks were associated with reduced attentional control costs. Again, these relationships were also consistent after controlling for Trails A performance. Furthermore, SVR prediction of the attention composite was consistently successful, although somewhat reduced, after correcting for CVH both before (R^2 = .062, p = .041) and after (R^2 = .093, p = .012) additionally correcting for processing speed (see Table 3). Hence, although cognitive relationships with resting-state BOLD variability may be influenced by CVH, attentional control relationships with task-driven variability remain after correcting for these measures and, thus, may be sensitive to distinct sources of variance.

Relationships with In-scanner Task Performance

Moving beyond the cognitive composite estimates, which were collected in a separate session from the resting-state and task-driven fMRI sessions, we also evaluated whether BOLD *SD* was sensitive to behavioral performance in tasks completed within the fMRI scanner. Because the attentional control composite (which notably included a different Stroop task) was particularly related to BOLD *SD* during both resting-state and task-driven blocks, we focused on relationships with Stroop performance in the task-driven fMRI session. Although the composite measures operationalized attentional control using difference score costs in RT, as noted, these estimates are less reliable than simpler point estimates (Lord, 1956). The composite score approach we used might successfully compensate for the low reliability of difference score estimates when multiple attentional control tasks are available, but this approach is limited in the case of in-scanner task performance, because participants only completed a single Stroop task and an animacy judgment task. Hence, to improve the reliability of our in-scanner behavioral estimate, we focused on the average standardized RT (ZRT) of incongruent Stroop trials only. By standardizing incongruent RT in *SD* units above or below a participant's overall mean RT, this measure also corrects for individual differences in overall processing speed (Faust, Balota, Spieler, & Ferraro, 1999).

Indeed, as shown in Figure 6A, we observed negative relationships such that greater task-driven BOLD *SD* was associated with less relative slowing on incongruent Stroop trials (i.e., faster Stroop incongruent ZRT). Specifically, marginal negative relationships were observed in SM, VIS, and DAN networks. These relationships in the VIS and DAN networks are consistent with the networks in which task-driven BOLD *SD* was found to relate to attentional composite estimates. Furthermore, as shown in Figure 6B, SVR models were marginally successful in predicting incongruent Stroop ZRT from task-driven BOLD *SD* (R^2 = .051, p = .057).

Again, we evaluated the multivariate relationship between incongruent Stroop ZRT and task-driven BOLD *SD* in terms of specific networks using network-driven feature selection. As shown in Figure 3D, BOLD *SD* estimates within the VIS network (R^2 = .172) were particularly successful in predicting incongruent ZRT, compared to other networks, and significantly outperformed a matched bootstrapped distribution (empirical p = .014). SVR performance from other networks fell within the range expected by randomly selected regions (empirical ps ≥ .251). Hence, the multivariate relationship between task-driven BOLD *SD* and incongruent Stroop ZRT might be particularly strong in the VIS network but is otherwise widely distributed throughout networks.[7]

Importantly, the correlations with incongruent Stroop ZRT also remain after correction for age or CVH. As shown in Figure 6C and E, marginal negative relationships with Stroop performance were observed in consistent networks after controlling for age and CVH. Furthermore, SVR models were marginally successful in predicting incongruent Stroop ZRT after correcting for age (R^2 = .052, p = .054), although they were unsuccessful after controlling for CVH (R^2 = .019, p = .246).

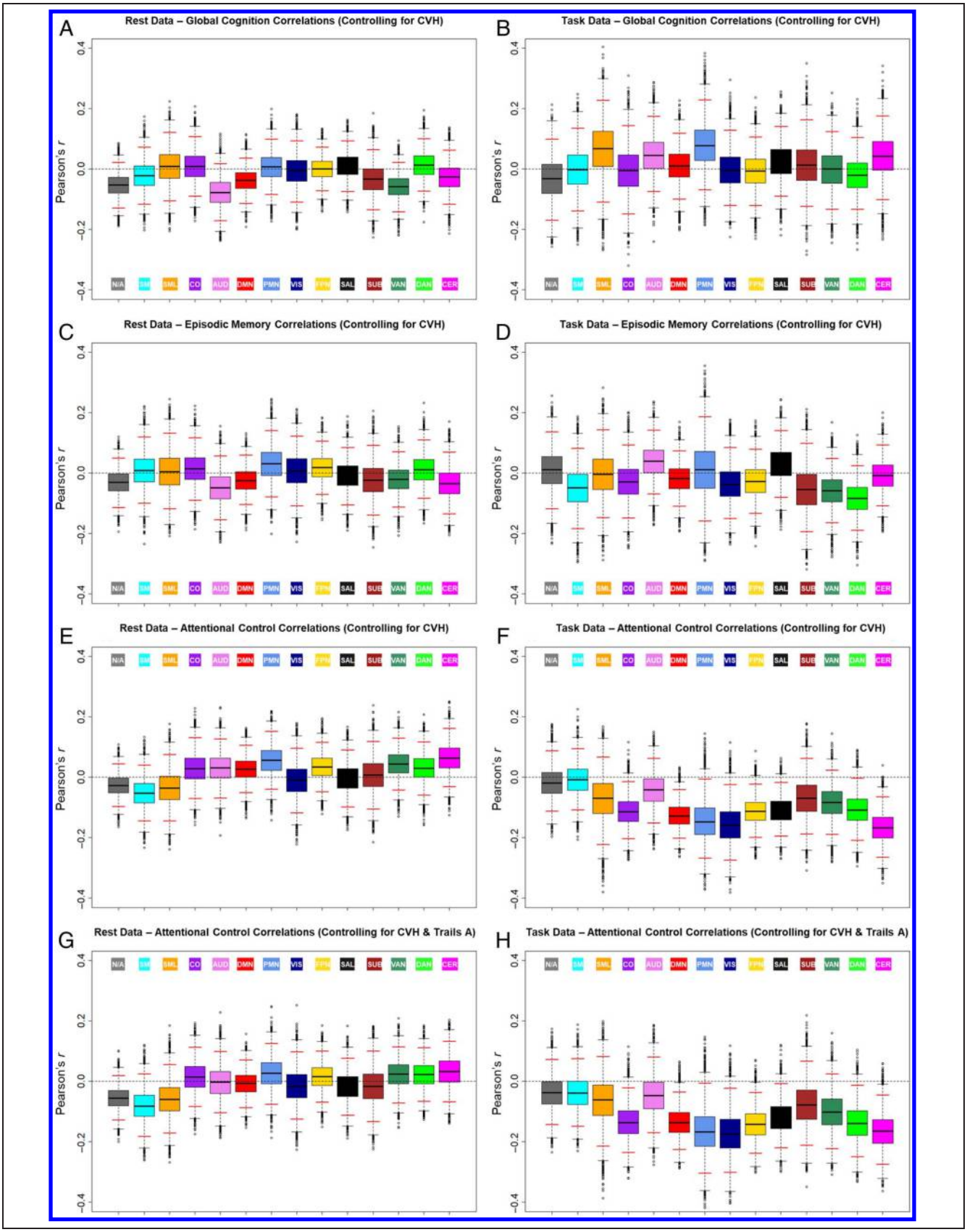

Figure 5. Boxplots of the distribution and 95% confidence interval (red lines) of bootstrapped distributions of network average Pearson correlations between BOLD *SD* and global cognition (A and B), episodic memory (C and D), attentional control (E and F), and attentional control corrected for Trails A (G and H) after controlling for CVH measures. Relationships are shown for both resting-state (left column; A, C, E, and G) and task-driven (right column; B, D, F, and H) fMRI sessions. Distributions in which the 95% confidence interval (red lines) excludes 0 (dotted black line) reflect significant network-level relationships.

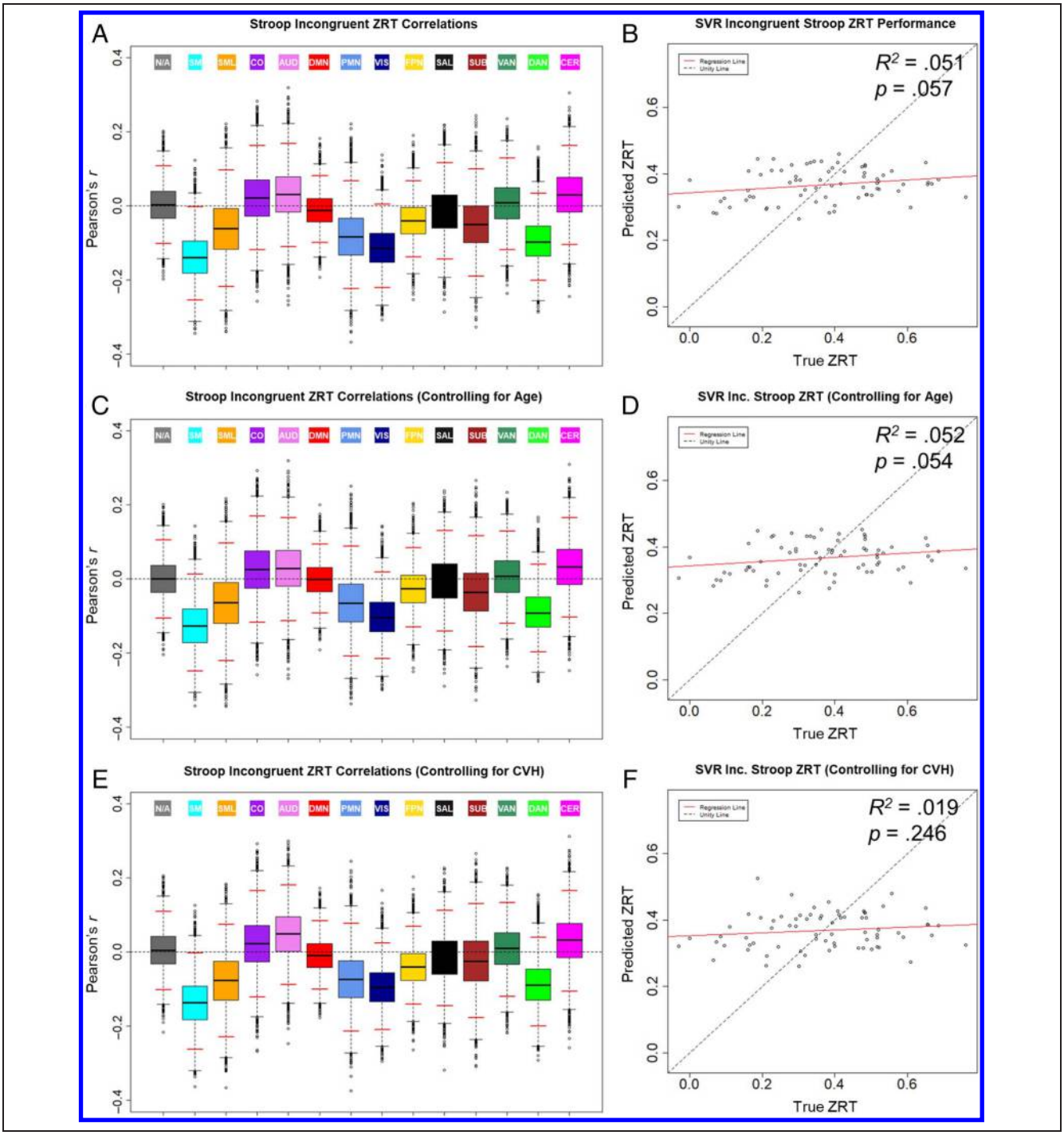

Figure 6. Relationships between task-driven BOLD *SD* and in-scanner incongruent (Inc.) Stroop ZRT. Boxplots (left column; A, C, and E) display the distribution and empirical 95% confidence interval (red lines) of bootstrapped distributions of network average Pearson correlations. Scatterplots (right column; B, D, and F) display in-scanner behavioral measures predicted by SVR model as a function of true score. Relationships are shown for uncorrected BOLD *SD* (A and B), as well as after controlling for age (C and D) and CVH estimates' composite (E and F).

Finally, one possible interpretation of task-driven BOLD *SD* is that these estimates might largely capture task event-related modulations in the BOLD signal evoked by the task stimuli and performance. Thus, it is unclear whether task-driven BOLD *SD* might capture distinct fluctuations that are not captured in a traditional contrast comparison or event-related model of task activation. To examine this possibility, we tested the relationships between incongruent Stroop ZRT and task-driven BOLD variability after regressing the task event model from the BOLD time series data. Specifically, we included timing parameters for the event-related design of each trial type as nuisance regressors during BOLD preprocessing.

As shown in Figure 7A, negative relationships between incongruent Stroop ZRT and BOLD *SD* were observed in consistent networks after controlling for the task event model. SVR models were still able to marginally predict Stroop performance (R^2 = .047, p = .069; see Figure 7B). Moreover, the network-level correlations and SVR performance were largely unchanged in estimates of task-driven BOLD *SD* corrected for age (see Figure 7C and D) and CVH (see Figure 7E and F). Hence, task-driven BOLD *SD* may capture task-relevant fluctuations in the BOLD signal that are distinct from task-related events.

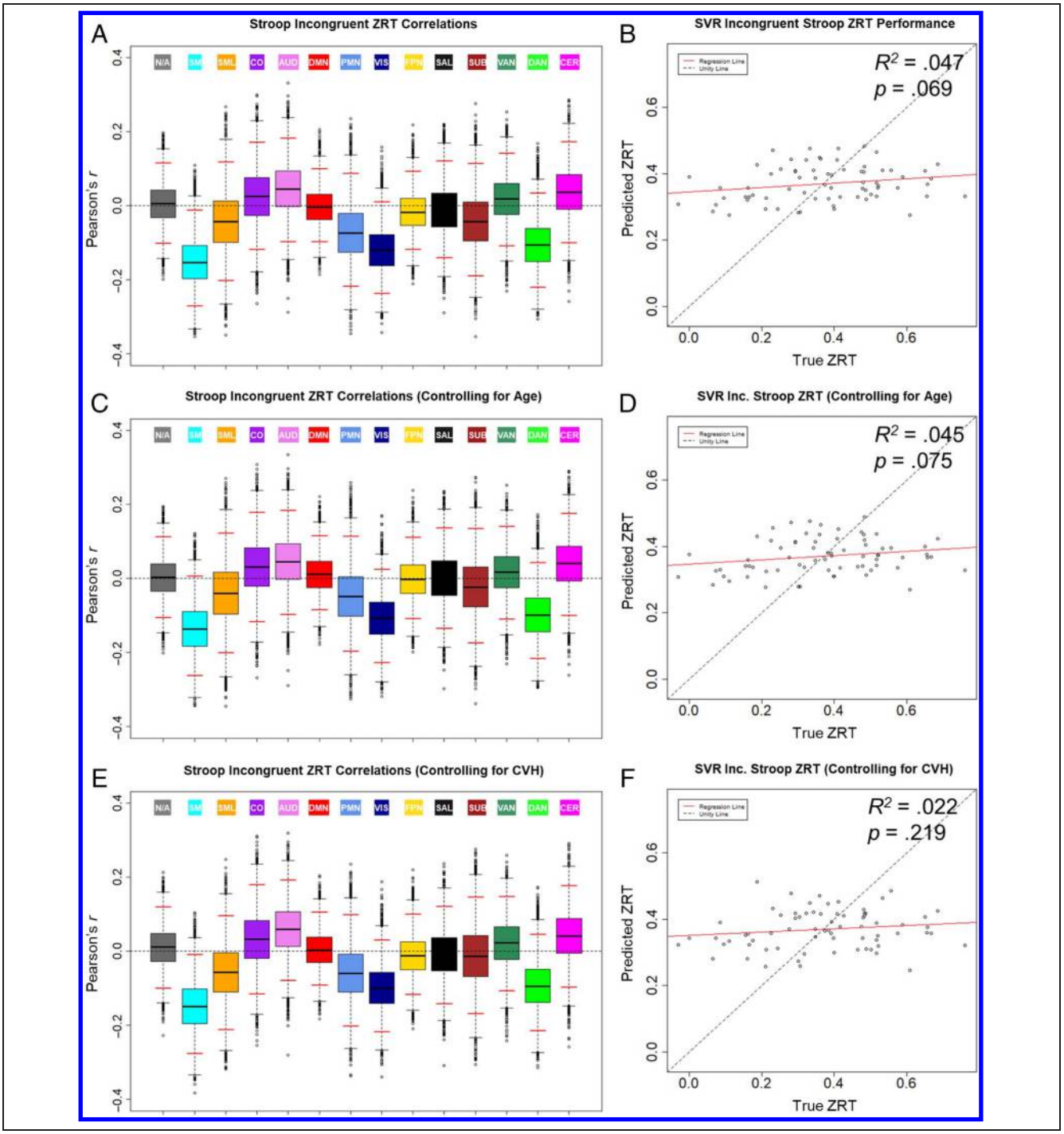

Figure 7. Relationships between task-driven BOLD *SD* and in-scanner incongruent (Inc.) Stroop ZRT after regressing out the model of task-related events. Boxplots (left column; A, C, and E) display the distribution and empirical 95% confidence interval (red lines) of bootstrapped distributions of network average Pearson correlations. Scatterplots (right column; B, D, and F) display in-scanner behavioral measures predicted by SVR model as a function of true score. Relationships are shown for uncorrected BOLD *SD* (A and B) as well as after controlling for age (C and D) and CVH estimates (E and F).

DISCUSSION

This study offers several noteworthy findings. First, we demonstrated that BOLD variability was greater during resting-state than during task-driven scans. Second, resting-state BOLD variability (but not task-driven BOLD variability) was related to better performance on a global cognitive composite measured outside the scanner. Third, BOLD variability estimates during both resting-state and task-driven runs were related to composite estimates of costs of attentional control demands. Fourth, task-driven BOLD variability was similarly related with less attentional control on in-scanner Stroop performance. Finally, the attentional relationships with task-driven BOLD variability remained after correction for age or CVH, whereas attentional and global cognitive relationships with resting-state variability did not. We now discuss each of these findings in turn, as we focus on interpretations of BOLD variability as a potential signal in relation to cognition, as well as how these findings extend upon previous reports in the literature.

Comparison of Resting-State vs. Task-Driven BOLD Variability

We observed significant modulations in BOLD variability estimates, such that variability was greater during resting-state than during task-driven runs. In addition, BOLD variability during brief fixation blocks was significantly greater than variability during task performance. Thus, the present results consistently suggest that variability is elevated in off-task states during both relatively short (30 sec) and long (360 sec) timescales. These results conflict with recent reports that task-driven BOLD variability is increased in comparison to resting-state (Grady & Garrett, 2018; Garrett, Kovacevic, et al., 2013). Rather, the direction of the present result is more consistent with earlier demonstrations that task-driven BOLD variability and spontaneous activity are reduced during task performance (He, 2011; Bianciardi et al., 2009; Fransson, 2006). The direction of this effect might be explained by a negative interaction between spontaneous and task-evoked activity, such that greater spontaneous activity at baseline might be associated with reduced task activation (He, 2013). However, this effect might also be influenced by other factors, including the type of behavioral task performed, the timing of task-related events, and the sequential ordering of resting-state, task-driven, and fixation blocks. Hence, additional studies should further examine the influence of task performance on regional estimates of BOLD variability. Furthermore, we also found that BOLD variability estimates were highly correlated across different tasks, but correlations were surprisingly low between task-driven and resting-state estimates. Together, these patterns suggest that task-driven BOLD variability estimates may be sensitive to distinct sources of variance from resting-state estimates and that these signals may be relatively consistent across tasks.

Behavioral Sensitivity of BOLD Variability

Global Cognition

Consistent with recent findings in a mostly overlapping sample (Millar, Petersen, et al., 2020), performance on a global cognitive composite of episodic memory (FSCR free recall), semantic fluency (Animal Naming), processing speed (Trail Making A), and executive function (Trail Making B) was associated with resting-state BOLD variability. The multivariate pattern of variability across networks captured a small, but significant, portion of variance in global cognition. Importantly, however, multivariate prediction of global cognition from individual networks did not outperform matched, randomly selected regions. Hence, associations between resting-state BOLD variability and global cognition are likely supported by a mechanism spread diffusely across functional networks.

However, relationships with global cognition did not replicate in a task-driven fMRI subsample. This difference was consistent after quantifying and controlling for differences in the time interval between behavioral task batteries and the resting-state and task-driven fMRI sessions (see Footnote 6). It is possible that BOLD variability during resting-state and task-driven runs might reflect qualitatively different signals. The presence of sensory input, demands of task performance, and motor responses likely elicit distinct sources of variance in the BOLD signal, which could augment or suppress spontaneous fluctuations observed during resting state. Under this view, the cognitive sensitivity of a BOLD variability estimate might change depending on the nature of the task being performed, as suggested by previous demonstrations of state-dependent modulations in BOLD variability (e.g., Grady & Garrett, 2018).

Episodic Memory

In comparison to measures of global cognition and attentional control, we found very little support for associations between BOLD variability and episodic memory. This result was surprising considering a prior demonstration that resting-state BOLD variability was positively associated with a factor estimate of similar episodic memory measures (including logical memory, free recall, and paired associate tasks) in a similar, large sample of cognitively normal older adults (Burzynska et al., 2015). However, it is noteworthy that the emphasis in this prior study was on voxel-level variability as opposed to network-level variability.

Attentional Control

The strongest behavioral relationships with BOLD variability were observed in measures of attentional control. Specifically, we found that smaller RT costs on a composite of attentional control tasks were associated with greater BOLD variability during both resting-state and task-driven runs in several sensory and association networks.

Interestingly, some of the most consistent and robust relationships with attentional control were observed in the VIS network. Notably, our composite measures of attentional control included all visually presented stimuli. Hence, greater variability in visual areas (either during resting-state or task-driven runs) may reflect more flexible or efficient processing of randomly presented visual inputs (e.g., color processing of Stroop trials). This finding is consistent with several other associations between resting-state or task-driven BOLD variability in visual areas and performance on visually mediated tasks (Grady & Garrett, 2018; Guitart-Masip et al., 2016; Burzynska et al., 2015; Garrett et al., 2011, 2014). Together, these results suggest that BOLD variability in visual areas is associated with more efficient processing of visual inputs, although it is unclear whether this relationship may be sensitive to mechanisms related to neural population coding of Bayesian optimal probability distributions (Ma et al., 2006), exploration of possible activation states (Deco et al., 2011), dynamic range of processing areas, or some other potential mechanisms.

Interestingly, although the attentional control composite was associated with BOLD variability in many of the same networks during resting-state and task-driven fMRI sessions, there were additional networks that only showed attentional relationships during task-driven runs: specifically the CO, DMN, DAN, VAN, and CER networks. Notably, many of these networks are associated with the initiation and maintenance of goal-directed attentional control as well as the detection of and orienting to salient stimuli (Dosenbach, Fair, Cohen, Schlaggar, & Petersen, 2008; Corbetta & Shulman, 2002). It is possible that variability in these networks might reflect modulation driven by control-related signals that were not elicited during the resting state. Under this interpretation, task-driven BOLD variability may offer qualitatively different insights into behaviorally relevant, network-level neural processing, compared to resting-state variability.

After correcting for individual differences in processing speed based on Trails A performance, relationships with task-driven BOLD variability estimates are highly consistent, although relationships with resting-state BOLD variability were clearly reduced. Specifically, the SVR prediction of attentional control was reduced by over 80% in comparison to the raw RT difference scores. Hence, multivariate relationships between resting-state BOLD variability and performance costs on the attentional control tasks may be sensitive in part to individual differences in processing speed (see Faust et al., 1999; Salthouse, 1996; Myerson, Hale, Wagstaff, Poon, & Smith, 1990). In contrast, relationships between attentional control and task-driven BOLD variability were robust to correction for processing speed. Thus, these task-driven estimates appear to be relatively sensitive to attentional selection processes above and beyond overall processing speed.

Beyond the attentional composite measures, greater task-driven BOLD variability was also associated with less slowing on incongruent Stroop trials completed in the scanner. These relationships were observed in similar networks that were related to the attentional composite estimates, including VIS and DAN networks, but with additional relationships in the SM network. As noted, we used a ZRT estimate of performance that expresses incongruent RT in *SD* units above or below the participant's mean RT and, thus, corrects for individual differences in processing speed. Hence, these associations with BOLD variability might be attributable to attentional control processes, beyond simple processing speed.

Sources of Variance in the BOLD Signal

Critically, we found that cognitive relationships with BOLD variability during resting state were eliminated after correcting for age or CVH, but in contrast, relationships with task-driven variability remained after correction for these factors. This inconsistency might suggest a qualitative distinction between the sources of variance captured by resting-state versus task-driven BOLD variability. Specifically, although resting-state BOLD variability indeed appears to be a behaviorally sensitive signal, this relationship might be limited to more general influences on cognition. For instance, resting-state BOLD variability may only be sensitive to global cognition or attentional control insofar as it is sensitive to age or CVH rather than neural processing. This interpretation would be consistent with recent demonstrations that age differences in resting-state BOLD variability may be sensitive, at least in part, to cardiovascular and neurovascular factors (Millar, Petersen, et al., 2020; Tsvetanov et al., 2015, 2019; but see Garrett et al., 2017). Moreover, these findings are also in line with proposals that vascular influences are an important factor in age-related cognitive decline (for a review, see Abdelkarim et al., 2019; Wåhlin & Nyberg, 2019; O'Brien et al., 2003).

In contrast, task-driven BOLD variability appears to be sensitive to additional sources of variance in the BOLD signal above and beyond age and CVH. Because the task-driven fMRI session included a Stroop task and an animacy judgment task, which both required a degree of sustained attention, it is possible that task-driven estimates of variability might capture functional neural processing specifically relevant for the engagement and maintenance of attentional control. Thus, estimates of BOLD variability during attentional task performance may be particularly sensitive to measures of attentional control both inside and outside the scanner and, furthermore, should be robust to individual differences in age and CVH. As noted, this interpretation also leads to the prediction that behavioral relationships with estimates of BOLD variability might vary depending on the cognitive demands of the task performed in the scanner, which is consistent with the present and previous demonstrations that BOLD variability change as a function of task demands (Grady & Garrett, 2018; Garrett et al., 2014).

Finally, we observed that relationships between task-driven BOLD variability and in-scanner Stroop performance were largely consistent after regressing out the task event model from BOLD time series data. This result is consistent with the proposal that the BOLD variability estimates capture distinct aspects of brain function beyond traditional mean-based task activation (Zhang et al., 2018). Furthermore, these correlations also remained after correction for age and CVH. Hence, task-driven BOLD variability, particularly in SM, VIS, and DAN networks, might be sensitive to behaviorally relevant sources of BOLD variance above and beyond task event-related responses and age-related or vascular factors.

Limitations and Future Directions

As noted, our results suggest that the behavioral relevance of BOLD variability estimates might vary depending on the nature of the task performed in the scanner. However, we examined a limited task-driven data set, which included only an animacy judgment task and a Stroop task. Future studies should explore these relationships using fMRI tasks that engage a broader range of cognitive domains. BOLD variability during these tasks might yield different patterns of behavioral sensitivity to measures of performance both inside and outside the scanner.

In addition, although resting-state and task-driven fMRI sessions were run (in most cases) on the same scanner and were processed through a matching pipeline, these sessions used different (but similar) functional imaging sequence parameters. Moreover, task-driven fMRI sessions were only run on a relatively small subset of the full resting-state fMRI cohort. Thus, a direct comparison between the resting-state and task-driven BOLD variability estimates derived from these samples should be interpreted with caution and should be further examined in matched data sets.

In contrast to this study, many other studies of BOLD variability have controlled for artifacts using independent component analysis (ICA) denoising. However, comparisons of processing pipelines have demonstrated that ICA is insufficient for removing motion-related artifacts in functional connectivity estimates, unless combined with GSR (Ciric et al., 2017). We have demonstrated that GSR is effective in minimizing motion relationships with BOLD *SD* estimates (Millar, Petersen, et al., 2020). However, no studies have directly compared the impact of ICA and GSR on estimates of BOLD variability (cf. Ciric et al., 2017). Hence, it is unclear whether behavioral relationships may be influenced by the choice of denoising procedures.

Finally, although we demonstrated that controlling for age or CVH eliminates behavioral relationships with resting-state BOLD variability, these analyses were limited to cross-sectional relationships among these variables. Thus, although the results are consistent with proposals that vascular influences may contribute to age-related cognitive decline (for a review, see Abdelkarim et al., 2019; Wåhlin & Nyberg, 2019; O'Brien et al., 2003), we cannot assume that they reflect causal contributions to cognitive relationships, as they may be simply driven by accounting for shared variance among the measures. For instance, cross-sectionally controlling for other age-related variables, such as bone density, might similarly reduce the relationships. Hence, the sensitivity of these brain–behavior relationships to broader age- and vascular-related mechanisms should be further examined in longitudinal samples.

Conclusions

In summary, this study supports the proposal that BOLD variability is a behaviorally sensitive signal. In particular, BOLD variability throughout a wide range of functional networks, including sensory, motor, and control networks, appears to be sensitive to performance on established measures of attentional control and, to some extent, global cognitive measures as well. However, our results also suggest important dissociations between resting-state and task-driven BOLD variability. Specifically, behavioral relationships with resting-state BOLD variability were not maintained after correcting for age or estimates of CVH, suggesting that these relationships may be sensitive to more general mechanisms. In contrast, behavioral relationships with task-driven BOLD variability remained after correction for these factors, suggesting that variability during task performance might be uniquely sensitive to distinct sources of variance above and beyond age and/or CVH. Of course, we can only draw limited interpretations regarding the contributions of age and CVH given the cross-sectional design (Lindenberger, von Oertzen, Ghisletta, & Hertzog, 2011), but future longitudinal designs might test these contributions more formally.

Acknowledgments

This research was funded by grants from the National Institutes of Health (P01-AG026276, P01-AG03991, P50-AG05681, R01-MH118031, R01-AG052550, R01-AG057680, T32-AG000030-41, 1S10RR022984-01A1, 1S10OD018091-01, and K01 AG053474), with generous support from the Paula and Rodger O. Riney Fund and the Daniel J. Brennan MD Fund. We thank the participants for their dedication to this project; the Knight Alzheimer Disease Research Center Psychometric Core for data collection; Jan Duchek, Doug Garrett, Denise Head, and Steve Petersen for helpful comments; Jo Etzel for consultation on support vector regression analyses; Dimitre Tomov for technical and programming support; and Julie Wisch for data curation support. Similar analyses of relationships between resting-state BOLD *SD* and the global cognitive composite in a mostly overlapping sample were recently reported in a manuscript in press at *Cerebral Cortex* (Millar, Petersen, et al.,2020).

Reprint requests should be sent to Peter R. Millar, Department of Neurology, Washington University in St. Louis, 660 S. Euclid Ave., Campus Box 8111, St. Louis, MO 63110, or via e-mail: pmillar@wustl.edu.

Funding Information

National Institutes of Health (http://dx.doi.org/10.13039/100000002), Grant number: 1S10OD018091-01, 1S10RR022984-01A1, K01 AG053474, P01-AG026276, P01-AG03991, P50-AG05681, R01-AG052550, R01-AG057680, R01-MH118031, T32-AG000030-41.

Notes

1. Although the correlations among attentional control estimates were relatively low compared to the global and episodic memory measures, this pattern is unsurprising because the attentional control tasks are based on difference scores, which are less reliable than point estimates (Lord, 1956). Thus, there should be a lower limit of expected correlations among the attentional control estimates than among the global or episodic memory measures, which were based on point estimates.
2. Visual examination of the CVH measures revealed that WMH estimates were highly skewed (see Figure 1C), and thus, cases in the tail of the distribution may disproportionately influence results when using WMH as a covariate. Thus, in addition to using the raw WMH volumes, we repeated the analyses using log-transformed WMH (Figure 1D) along with the other CVH covariates. Associations between BOLD variability and the cognitive composites were consistent for both the raw and log-transformed approaches (data not shown).
3. There were very strong correlations between estimates of BOLD *SD* derived from the complete usable time series and randomly selected frames (resting-state rs ≥ .989, task-driven rs ≥ .952) and between different random samples of frames (resting-state rs ≥ .978, task-driven rs ≥ .911). Thus, these randomly sampled frames are representative of variability present in the full time series.
4. The increased sensitivity of the task-driven variability estimates to head motion might be attributable to the ordering of the functional scans. Specifically, in most cases when resting-state and task-driven scans were performed in the same session, the resting-state scan preceded the task-driven scan. Thus, motion and its related artifacts might be more prominent in the task-driven scans because of greater participant fatigue.
5. By averaging the BOLD time series across voxels within each ROI, it is possible that variability in voxels that are out of phase will cancel each other out. Thus, in addition to the mean-based ROI approach, we also estimated variability in a concatenated time series of each individual voxel within the given ROIs. Regional variability estimates of the concatenated voxelwise ROI time series were very strongly correlated with variability estimates of the mean ROI time series for both resting-state (mean r = .979, range = .940–.996) and task-driven (mean r = .949, range = .874–.990) estimates. Hence, variability captured in the averaged ROI time series is largely representative of variability in the individual voxels.
6. One possible reason for the inconsistency between the resting-state and task-driven relationships is a difference in the time intervals between the global cognitive composite measures and the separate fMRI sessions. Indeed, the interval between the psychometric battery and the fMRI session was greater for the task session than it was for the resting-state session (t = 2.234, p = .026). Thus, the larger interval might introduce greater measurement error in any relationships between behavior and BOLD variability. Hence, for all cognitive composites, we additionally corrected for the signed interval between behavioral and fMRI sessions, which was standardized across resting-state and task-driven sessions, as a regressor of noninterest. All reliable behavioral relationships with resting-state and task-driven BOLD variability were consistent after controlling for the time interval.
7. Because we examined cognitive relationships with BOLD variability at the level of functional networks, it is possible that our results might be influenced by the set of ROIs and network assignment scheme. Thus, we additionally analyzed relationships with variability using an independent set of ROIs and network assignments (Shirer, Ryali, Rykhlevskaia, Menon, & Greicius, 2012). These results suggested that (i) correlations with cognitive measures were observed in corresponding networks between the two parcellations; (ii) SVR models identified consistent multivariate relationships with cognitive measures after controlling for age and CVH; and (iii) although there were some subtle differences in the multivariate network-level relationships identified using the two parcellation schemes, there was overall agreement that BOLD *SD* estimates in visual and visuospatial networks were particularly sensitive to attentional control estimates (data not shown). Hence, our primary conclusions from these analyses are supported by results using two independent network assignment schemes.

REFERENCES

Abdelkarim, D., Zhao, Y., Turner, M. P., Sivakolundu, D. K., Lu, H., & Rypma, B. (2019). A neural–vascular complex of age-related changes in the human brain: Anatomy, physiology, and implications for neurocognitive aging. *Neuroscience & Biobehavioral Reviews*, *107*, 927–944. **DOI:** https://doi.org/10.1016/j.neubiorev.2019.09.005, **PMID:** 31499083

Armitage, S. G. (1946). An analysis of certain psychological tests use for the evaluation of brain injury. *Psychological Monographs*, *60*, 1–48. **DOI:** https://doi.org/10.1037/h0093567

Aschenbrenner, A. J., Balota, D. A., Fagan, A. M., Duchek, J. M., Benzinger, T. L. S., & Morris, J. C. (2015). Alzheimer disease cerebrospinal fluid biomarkers moderate baseline differences and predict longitudinal change in attentional control and episodic memory composites in the Adult Children Study. *Journal of the International Neuropsychological Society*, *21*, 573–583. **DOI:** https://doi.org/10.1017/S1355617715000776, **PMID:** 26416094, **PMCID:** PMC4610253

Aschenbrenner, A. J., Gordon, B. A., Benzinger, T. L. S., Morris, J. C., & Hassenstab, J. J. (2018). Influence of tau PET, amyloid PET, and hippocampal volume on cognition in Alzheimer disease. *Neurology*, *91*, e859–e866. **DOI:** https://doi.org/10.1212/WNL.0000000000006075, **PMID:** 30068637, **PMCID:** PMC6133625

Balota, D. A., & Duchek, J. M. (2015). Attention, variability, and biomarkers in Alzheimer's disease. In D. S. Lindsay (Ed.), *Remembering: Attributions, processes, and control in human memory* (pp. 285–303). New York: Psychology Press.

Bianciardi, M., Fukunaga, M., van Gelderen, P., Horovitz, S. G., de Zwart, J. A., & Duyn, J. H. (2009). Modulation of spontaneous fMRI activity in human visual cortex by behavioral state. *Neuroimage*, *45*, 160–168. **DOI:** https://doi.org/10.1016/j.neuroimage.2008.10.034, **PMID:** 19028588, **PMCID:** PMC2704889

Brier, M. R., Thomas, J. B., Snyder, A. Z., Benzinger, T. L., Zhang, D., Raichle, M. E., et al. (2012). Loss of intranetwork and internetwork resting state functional connections with Alzheimer's disease progression. *Journal of Neuroscience*, *32*, 8890–8899. **DOI:** https://doi.org/10.1523/JNEUROSCI.5698-11.2012, **PMID:** 22745490, **PMCID:** PMC3458508

Burzynska, A. Z., Wong, C. N., Voss, M. W., Cooke, G. E., McAuley, E., & Kramer, A. F. (2015). White matter integrity supports BOLD signal variability and cognitive performance in the aging human brain. *PLoS One*, *10*, e0120315. **DOI:** https://doi.org/10.1371/journal.pone.0120315, **PMID:** 25853882, **PMCID:** PMC4390282

Castel, A. D., Balota, D. A., Hutchison, K. A., Logan, J. M., & Yap, M. J. (2007). Spatial attention and response control in healthy younger and older adults and individuals with Alzheimer's disease: Evidence for disproportionate selection impairments in the Simon task. *Neuropsychology*, *21*, 170–182. **DOI:** https://doi.org/10.1037/0894-4105.21.2.170, **PMID:** 17402817

Ciric, R., Wolf, D. H., Power, J. D., Roalf, D. R., Baum, G. L., Ruparel, K., et al. (2017). Benchmarking of participant-level confound regression strategies for the control of motion artifact in studies of functional connectivity. *Neuroimage*, *154*, 174–187. **DOI:** https://doi.org/10.1016/j.neuroimage.2017.03.020, **PMID:** 28302591, **PMCID:** PMC5483393

Clare Kelly, A. M., Uddin, L. Q., Biswal, B. B., Castellanos, F. X., & Milham, M. P. (2008). Competition between functional brain networks mediates behavioral variability. *Neuroimage*, *39*, 527–537. **DOI:** https://doi.org/10.1016/j.neuroimage.2007.08.008, **PMID:** 17919929

Corbetta, M., & Shulman, G. L. (2002). Control of goal-directed and stimulus-driven attention in the brain. *Nature Reviews Neuroscience*, *3*, 201–215. **DOI:** https://doi.org/10.1038/nrn755, **PMID:** 11994752

Crossman, E. R., & Szafran, J. (1956). Changes with age in the speed of information intake and discrimination. *Experientia*, *4*, 128–134. **PMID:** 13414745

Deco, G., Jirsa, V. K., & McIntosh, A. R. (2011). Emerging concepts for the dynamical organization of resting-state activity in the brain. *Nature Reviews Neuroscience*, *12*, 43–56. **DOI:** https://doi.org/10.1038/nrn2961, **PMID:** 21170073

Dosenbach, N. U. F., Fair, D. A., Cohen, A. L., Schlaggar, B. L., & Petersen, S. E. (2008). A dual-networks architecture of top–down control. *Trends in Cognitive Sciences*, *12*, 99–105. **DOI:** https://doi.org/10.1016/j.tics.2008.01.001, **PMID:** 18262825, **PMCID:** PMC3632449

Dosenbach, N. U. F., Nardos, B., Cohen, A. L., Fair, D. A., Power, J. D., Church, J. A., et al. (2010). Prediction of individual brain maturity using fMRI. *Science*, *329*, 1358–1361. **DOI:** https://doi.org/10.1126/science.1194144, **PMID:** 20829489, **PMCID:** PMC3135376

Duchek, J. M., Balota, D. A., Thomas, J. B., Snyder, A. Z., Rich, P., Benzinger, T. L., et al. (2013). Relationship between Stroop performance and resting state functional connectivity in cognitively normal older adults. *Neuropsychology*, *27*, 516–528. **DOI:** https://doi.org/10.1037/a0033402, **PMID:** 24040929, **PMCID:** PMC3837537

Fair, D. A., Schlaggar, B. L., Cohen, A. L., Miezin, F. M., Dosenbach, N. U. F., Wenger, K. K., et al. (2007). A method for using blocked and event-related fMRI data to study "resting state" functional connectivity. *Neuroimage*, *35*, 396–405. **DOI:** https://doi.org/10.1016/j.neuroimage.2006.11.051, **PMID:** 17239622, **PMCID:** PMC2563954

Faust, M. E., Balota, D. A., Spieler, D. H., & Ferraro, F. R. (1999). Individual differences in information-processing rate and amount: Implications for group differences in response latency. *Psychological Bulletin*, *125*, 777–799. **DOI:** https://doi.org/10.1037/0033-2909.125.6.777, **PMID:** 10589302

Fischl, B. (2012). FreeSurfer. *Neuroimage*, *62*, 774–781. **DOI:** https://doi.org/10.1016/j.neuroimage.2012.01.021, **PMID:** 22248573, **PMCID:** PMC3685476

Fox, M. D., & Raichle, M. E. (2007). Spontaneous fluctuations in brain activity observed with functional magnetic resonance imaging. *Nature Reviews Neuroscience*, *8*, 700–711. **DOI:** https://doi.org/10.1038/nrn2201, **PMID:** 17704812

Fox, M. D., Zhang, D., Snyder, A. Z., & Raichle, M. E. (2009). The global signal and observed anticorrelated resting state brain networks. *Journal of Neurophysiology*, *101*, 3270–3283. **DOI:** https://doi.org/10.1152/jn.90777.2008, **PMID:** 19339462, **PMCID:** PMC2694109

Fransson, P. (2006). How default is the default mode of brain function?: Further evidence from intrinsic BOLD signal fluctuations. *Neuropsychologia*, *44*, 2836–2845. **DOI:** https://doi.org/10.1016/j.neuropsychologia.2006.06.017, **PMID:** 16879844

Garrett, D. D., Epp, S. M., Perry, A., & Lindenberger, U. (2018). Local temporal variability reflects functional integration in the human brain. *Neuroimage*, *183*, 776–787. **DOI:** https://doi.org/10.1016/j.neuroimage.2018.08.019, **PMID:** 30149140

Garrett, D. D., Kovacevic, N., McIntosh, A. R., & Grady, C. L. (2010). Blood oxygen level-dependent signal variability is more than just noise. *Journal of Neuroscience*, *30*, 4914–4921. **DOI:** https://doi.org/10.1523/JNEUROSCI.5166-09.2010, **PMID:** 20371811, **PMCID:** PMC6632804

Garrett, D. D., Kovacevic, N., McIntosh, A. R., & Grady, C. L. (2011). The importance of being variable. *Journal of Neuroscience*, *31*, 4496–4503. **DOI:** https://doi.org/10.1523/JNEUROSCI.5641-10.2011, **PMID:** 21430150, **PMCID:** PMC3104038

Garrett, D. D., Kovacevic, N., McIntosh, A. R., & Grady, C. L. (2013). The modulation of BOLD variability between cognitive states varies by age and processing speed. *Cerebral Cortex*, *23*, 684–693. **DOI:** https://doi.org/10.1093/cercor/bhs055, **PMID:** 22419679, **PMCID:** PMC3823571

Garrett, D. D., Lindenberger, U., Hoge, R. D., & Gauthier, C. J. (2017). Age differences in brain signal variability are robust to multiple vascular controls. *Scientific Reports*, *7*, 10149. **DOI:** https://doi.org/10.1038/s41598-017-09752-7, **PMID:** 28860455, **PMCID:** PMC5579254

Garrett, D. D., McIntosh, A. R., & Grady, C. L. (2014). Brain signal variability is parametrically modifiable. *Cerebral Cortex*, *24*, 2931–2940. **DOI:** https://doi.org/10.1093/cercor/bht150, **PMID:** 23749875, **PMCID:** PMC4193462

Garrett, D. D., Nagel, I. E., Preuschhof, C., Burzynska, A. Z., Marchner, J., Wiegert, S., et al. (2015). Amphetamine modulates brain signal variability and working memory in younger and older adults. *Proceedings of the National Academy of Sciences, U.S.A.*, *112*, 7593–7598. **DOI:** https://doi.org/10.1073/pnas.1504090112, **PMID:** 26034283, **PMCID:** PMC4475975

Garrett, D. D., Samanez-Larkin, G. R., MacDonald, S. W. S., Lindenberger, U., McIntosh, A. R., & Grady, C. L. (2013). Moment-to-moment brain signal variability: A next frontier in human brain mapping? *Neuroscience & Biobehavioral Reviews*, *37*, 610–624. **DOI:** https://doi.org/10.1016/j.neubiorev.2013.02.015, **PMID:** 23458776, **PMCID:** PMC3732213

Good, T. J., Villafuerte, J., Ryan, J. D., Grady, C. L., & Barense, M. D. (2020). Resting state bold variability of the posterior medial temporal lobe correlates with cognitive performance in older adults with and without risk for cognitive decline. *eNeuro*, 7. **DOI:** https://doi.org/10.1523/ENEURO.0290-19.2020, **PMID:** 32193364, PMCID: PMC7240288

Goodglass, H., & Kaplan, E. (1983). *Boston diagnostic aphasia examination booklet, III: Oral expression: Animal naming (Fluency in controlled association)*. Philadelphia: Lea & Febiger.

Gordon, B. A., Zacks, J. M., Blazey, T., Benzinger, T. L. S., Morris, J. C., Fagan, A. M., et al. (2015). Task-evoked fMRI changes in attention networks are associated with preclinical Alzheimer's disease biomarkers. *Neurobiology of Aging*, *36*, 1771–1779. **DOI:** https://doi.org/10.1016/j.neurobiolaging.2015.01.019, **PMID:** 25708908, **PMCID:** PMC4417039

Grady, C. L., & Garrett, D. D. (2014). Understanding variability in the BOLD signal and why it matters for aging. *Brain Imaging and Behavior*, *8*, 274–283. **DOI:** https://doi.org/10.1007/s11682-013-9253-0, **PMID:** 24008589, **PMCID:** PMC3922711

Grady, C. L., & Garrett, D. D. (2018). Brain signal variability is modulated as a function of internal and external demand in younger and older adults. *Neuroimage*, *169*, 510–523. **DOI:**

https://doi.org/10.1016/j.neuroimage.2017.12.031, **PMID:** 29253658

Gratton, C., Laumann, T. O., Nielsen, A. N., Greene, D. J., Gordon, E. M., Gilmore, A. W., et al. (2018). Functional brain networks are dominated by stable group and individual factors, not cognitive or daily variation. *Neuron*, *98*, 439–452. **DOI:** https://doi.org/10.1016/j.neuron.2018.03.035, **PMID:** 29673485, **PMCID:** PMC5912345

Grober, E., Buschke, H., Crystal, H., Bang, S., & Dresner, R. (1988). Screening for dementia by memory testing. *Neurology*, *38*, 900–903. **DOI:** https://doi.org/10.1212/WNL.38.6.900, **PMID:** 3368071

Guitart-Masip, M., Salami, A., Garrett, D. D., Rieckmann, A., Lindenberger, U., & Bäckman, L. (2016). BOLD variability is related to dopaminergic neurotransmission and cognitive aging. *Cerebral Cortex*, *26*, 2074–2083. **DOI:** https://doi.org/10.1093/cercor/bhv029, **PMID:** 25750252

He, B. J. (2011). Scale-free properties of the functional magnetic resonance imaging signal during rest and task. *Journal of Neuroscience*, *31*, 13786–13795. **DOI:** https://doi.org/10.1523/JNEUROSCI.2111-11.2011, **PMID:** 21957241, **PMCID:** PMC3197021

He, B. J. (2013). Spontaneous and task-evoked brain activity negatively interact. *Journal of Neuroscience*, *33*, 4672–4682. **DOI:** https://doi.org/10.1523/JNEUROSCI.2922-12.2013, **PMID:** 23486941, **PMCID:** PMC3637953

Honey, C. J., Kötter, R., Breakspear, M., & Sporns, O. (2007). Network structure of cerebral cortex shapes functional connectivity on multiple time scales. *Proceedings of the National Academy of Sciences, U.S.A.*, *104*, 10240–10245. **DOI:** https://doi.org/10.1073/pnas.0701519104, **PMID:** 17548818, **PMCID:** PMC1891224

Hu, S., Chao, H. H.-A., Zhang, S., Ide, J. S., & Li, C.-S. R. (2014). Changes in cerebral morphometry and amplitude of low-frequency fluctuations of BOLD signals during healthy aging: Correlation with inhibitory control. *Brain Structure and Function*, *219*, 983–994. **DOI:** https://doi.org/10.1007/s00429-013-0548-0, **PMID:** 23553547, **PMCID:** PMC3760988

Huff, M. J., Balota, D. A., Minear, M., Aschenbrenner, A. J., & Duchek, J. M. (2015). Dissociative global and local task-switching costs across younger adults, middle-aged adults, older adults, and very mild Alzheimer's disease individuals. *Psychology and Aging*, *30*, 727–739. **DOI:** https://doi.org/10.1037/pag0000057, **PMID:** 26652720, **PMCID:** PMC4681312

Kielar, A., Deschamps, T., Chu, R. K. O., Jokel, R., Khatamian, Y. B., Chen, J. J., et al. (2016). Identifying dysfunctional cortex: Dissociable effects of stroke and aging on resting state dynamics in MEG and fMRI. *Frontiers in Aging Neuroscience*, *8*, 40. **DOI:** https://doi.org/10.3389/fnagi.2016.00040, **PMID:** 26973515, **PMCID:** PMC4776400

Lindenberger, U., von Oertzen, T., Ghisletta, P., & Hertzog, C. (2011). Cross-sectional age variance extraction: What's change got to do with it? *Psychology and Aging*, *26*, 34–47. **DOI:** https://doi.org/10.1037/a0020525, **PMID:** 21417539

Lord, F. M. (1956). The measurement of growth. *ETS Research Bulletin Series*, *1956*, 1–22. **DOI:** https://doi.org/10.1002/j.2333-8504.1956.tb00058.x

Ma, W. J., Beck, J. M., Latham, P. E., & Pouget, A. (2006). Bayesian inference with probabilistic population codes. *Nature Neuroscience*, *9*, 1432–1438. **DOI:** https://doi.org/10.1038/nn1790, **PMID:** 17057707

Meeker, K. L., Ances, B. M., Gordon, B. A., Rudolph, C. W., Luckett, P., Balota, D. A., et al. (in press). Effects of CSF Aβ42 on brain functional network dynamics and cognitive intra-individual variability. *Neurobiology of Aging*. **DOI:** https://doi.org/10.1016/j.neurobiolaging.2020.10.027

Mennes, M., Zuo, X.-N., Clare Kelly, A. M., Di Martino, A., Zang, Y.-F., Biswal, B. B., et al. (2011). Linking inter-individual differences in neural activation and behavior to intrinsic brain dynamics. *Neuroimage*, *54*, 2950–2959. **DOI:** https://doi.org/10.1016/j.neuroimage.2010.10.046, **PMID:** 20974260, **PMCID:** PMC3091620

Meyer, D., Dimitriadou, E., Hornik, K., Weingessel, A., Leisch, F., Chang, C.-C., et al. (2017). Misc functions of the department of statistics, probability theory group (E1071), TU Wien. In *The Comprehensive R Archive Network* Retrieved from https://cran.r-project.org/web/packages/e1071/e1071.pdf

Millar, P. R., Ances, B. M., Gordon, B. A., Benzinger, T. L. S., Fagan, A. M., Morris, J. C., & Balota, D. A. (2020). Evaluating resting-state BOLD variability in relation to biomarkers of preclinical Alzheimer's disease. *Neurobiology of Aging*, *96*, 233–245. **DOI:** https://doi.org/10.1016/j.neurobiolaging.2020.08.007. **PMID:** 33039901

Millar, P. R., Petersen, S. E., Ances, B. M., Gordon, B. A., Benzinger, T. L. S., Morris, J. C., et al. (2020). Evaluating the sensitivity of resting-state BOLD variability to age and cognition after controlling for motion and cardiovascular influences: A network-based approach. *Cerebral Cortex*, *30*, 5686–5701. **DOI:** https://doi.org/10.1093/cercor/bhaa138, **PMID:** 32515824

Morris, J. C. (1993). The Clinical Dementia Rating (CDR): Current version and scoring rules. *Neurology*, *43*, 2412–2414. **DOI:** https://doi.org/10.1212/WNL.43.11.2412-a, **PMID:** 8232972

Myerson, J., Hale, S., Wagstaff, D., Poon, L. W., & Smith, G. A. (1990). The information-loss model: A mathematical theory of age-related cognitive slowing. *Psychological Review*, *97*, 475–487. **DOI:** https://doi.org/10.1037/0033-295X.97.4.475, **PMID:** 2247538

Nielsen, A. N., Barch, D. M., Petersen, S. E., Schlaggar, B. L., & Greene, D. J. (2020). Machine learning with neuroimaging: Evaluating its applications in psychiatry. *Biological Psychiatry: Cognitive Neuroscience and Neuroimaging*, *5*, 791–798. **DOI:** https://doi.org/10.1016/j.bpsc.2019.11.007, **PMID:** 31982357

Nielsen, A. N., Greene, D. J., Gratton, C., Dosenbach, N. U. F., Petersen, S. E., & Schlaggar, B. L. (2019). Evaluating the prediction of brain maturity from functional connectivity after motion artifact denoising. *Cerebral Cortex*, *29*, 2455–2469. **DOI:** https://doi.org/10.1093/cercor/bhy117, **PMID:** 29850877, **PMCID:** PMC6519700

Nomi, J. S., Bolt, T. S., Ezie, C. E. C., Uddin, L. Q., & Heller, A. S. (2017). Moment-to-moment BOLD signal variability reflects regional changes in neural flexibility across the lifespan. *Journal of Neuroscience*, *37*, 5539–5548. **DOI:** https://doi.org/10.1523/JNEUROSCI.3408-16.2017, **PMID:** 28473644, **PMCID:** PMC5452342

O'Brien, J. T., Erkinjuntti, T., Reisberg, B., Roman, G., Sawada, T., Pantoni, L., et al. (2003). Vascular cognitive impairment. *Lancet Neurology*, *2*, 89–98. **DOI:** https://doi.org/10.1016/S1474-4422(03)00305-3

Power, J. D., Barnes, K. A., Snyder, A. Z., Schlaggar, B. L., & Petersen, S. E. (2012). Spurious but systematic correlations in functional connectivity MRI networks arise from subject motion. *Neuroimage*, *59*, 2142–2154. **DOI:** https://doi.org/10.1016/j.neuroimage.2011.10.018, **PMID:** 22019881, **PMCID:** PMC3254728

Power, J. D., Cohen, A. L., Nelson, S. M., Wig, G. S., Barnes, K. A., Church, J. A., et al. (2011). Functional network organization of the human brain. *Neuron*, *72*, 665–678. **DOI:** https://doi.org/10.1016/j.neuron.2011.09.006, **PMID:** 22099467, **PMCID:** PMC3222858

Salthouse, T. A. (1996). The processing-speed theory of adult age differences in cognition. *Psychological Review*, *103*, 403–428. **DOI:** https://doi.org/10.1037/0033-295X.103.3.403, **PMID:** 8759042

Schmidt, P., Gaser, C., Arsic, M., Buck, D., Förschler, A., Berthele, A., et al. (2012). An automated tool for detection of FLAIR-hyperintense white-matter lesions in multiple sclerosis. *Neuroimage*, *59*, 3774–3783. **DOI:** https://doi.org/10.1016/j.neuroimage.2011.11.032, **PMID:** 22119648

Seitzman, B. A., Gratton, C., Marek, S., Raut, R. V., Dosenbach, N. U. F., Schlaggar, B. L., et al. (2020). A set of functionally-defined brain regions with improved representation of the subcortex and cerebellum. *Neuroimage*, *206*, 116290. **DOI:** https://doi.org/10.1016/j.neuroimage.2019.116290, **PMID:** 31634545

Shirer, W. R., Ryali, S., Rykhlevskaia, E., Menon, V., & Greicius, M. D. (2012). Decoding subject-driven cognitive states with whole-brain connectivity patterns. *Cerebral Cortex*, *22*, 158–165. **DOI:** https://doi.org/10.1093/cercor/bhr099, **PMID:** 21616982, **PMCID:** PMC3236795

Shulman, G. L., Pope, D. L. W., Astafiev, S. V., McAvoy, M. P., Snyder, A. Z., & Corbetta, M. (2010). Right hemisphere dominance during spatial selective attention and target detection occurs outside the dorsal frontoparietal network. *Journal of Neuroscience*, *30*, 3640–3651. **DOI:** https://doi.org/10.1523/JNEUROSCI.4085-09.2010, **PMID:** 20219998, **PMCID:** PMC2872555

Simon, J. R. (1969). Reactions toward the source of stimulation. *Journal of Experimental Psychology*, *81*, 174–176. **DOI:** https://doi.org/10.1037/h0027448, **PMID:** 5812172

Spieler, D. H., Balota, D. A., & Faust, M. E. (1996). Stroop performance in healthy younger and older adults and in individuals with dementia of the Alzheimer's type. *Journal of Experimental Psychology: Human Perception and Performance*, *22*, 461–479. **DOI:** https://doi.org/10.1037/0096-1523.22.2.461, **PMID:** 8934854

Stroop, J. R. (1935). Studies of interference in serial verbal reactions. *Journal of Experimental Psychology*, *18*, 643–662. **DOI:** https://doi.org/10.1037/h0054651

Tsvetanov, K. A., Henson, R. N. A., Jones, P. S., Mutsaerts, H.-J., Fuhrmann, D., Tyler, L. K., et al. (2019). The effects of age on resting-state BOLD signal variability is explained by cardiovascular and neurovascular factors. *BioRxiv*, 836619. **DOI:** https://doi.org/10.1101/836619

Tsvetanov, K. A., Henson, R. N. A., Tyler, L. K., Davis, S. W., Shafto, M. A., Taylor, J. R., et al. (2015). The effect of ageing on fMRI: Correction for the confounding effects of vascular reactivity evaluated by joint fMRI and MEG in 335 adults. *Human Brain Mapping*, *36*, 2248–2269. **DOI:** https://doi.org/10.1002/hbm.22768, **PMID:** 25727740, **PMCID:** PMC4730557

Wåhlin, A., & Nyberg, L. (2019). At the heart of cognitive functioning in aging. *Trends in Cognitive Sciences*, *23*, 717–720. **DOI:** https://doi.org/10.1016/j.tics.2019.06.004, **PMID:** 31303538

Wechsler, D. (1987). *Manual: Wechler memory scale-revised*. San Antonio, TX: Psychological Corporation.

Wechsler, D. (1997). *Manual: Wechsler adult intelligence scale-III*. New York: Psychological Corporation **DOI:** https://doi.org/10.1037/t49755-000

Wechsler, D., & Stone, C. P. (1973). *Manual: Wechsler Memory Scale*. New York: Psychological Corporation.

Wolf, D., Zschutschke, L., Scheurich, A., Schmitz, F., Lieb, K., Tüscher, O., et al. (2014). Age-related increases in Stroop interference: Delineation of general slowing based on behavioral and white matter analyses. *Human Brain Mapping*, *35*, 2448–2458. **DOI:** https://doi.org/10.1002/hbm.22340, **PMID:** 24038539, **PMCID:** PMC6869565

Zhang, L., Zuo, X., Ng, K. K., Su, J., Chong, X., Shim, H. Y., et al. (2020). Distinct BOLD variability changes in the default mode and salience networks in Alzheimer's disease spectrum and associations with cognitive decline. *Scientific Reports*, *10*, 6457. **DOI:** https://doi.org/10.1038/s41598-020-63540-4, **PMID:** 32296093, **PMCID:** PMC7160203

Zhang, P.-W., Qu, X.-J., Qian, S.-F., Wang, X.-B., Wang, R.-D., Li, Q.-Y., et al. (2018). Distinction between variability-based modulation and mean-based activation revealed by BOLD-fMRI and eyes-open/eyes-closed contrast. *Frontiers in Neuroscience*, *12*, 516. **DOI:** https://doi.org/10.3389/fnins.2018.00516, **PMID:** 30108478, **PMCID:** PMC6079296